aspects of photodynamic therapy (PDT). It is still not clear whether singlet molecular oxygen, O_2 (energy-transfer product, type II mechanism), superoxide radical, $O_2^{\bullet-}$ (electron-transfer product, type I mechanism), or a redox product of the sensitizer itself is the active species in the selective treatment of tumors by PDT. The oxidation and reduction potentials of the sensitizer are important variables in studies aimed at uncovering the mechanistic details of this process. The texaphyrin family of complexes provides an excellent opportunity for carrying out such mechanistic investigations.

Acknowledgment. This work was supported by Grant No. 1581 from the Texas Advanced Research Program to J.L.S and by a grant from the Division of Chemical Sciences, Office of Basic Energy Sciences, Department of Energy, under Contract DE-FG05-87ER13789 to T.E.M., J.L.S. and T.E.M. also thank the NSF for Presidental Young Investigator Awards, the Alfred P. Sloan Foundation for Research Fellowships, and the Camille and Henry Dreyfus Foundation for Teacher-Scholar Awards. Grateful acknowledgment is also made to the Midwest Center for Mass Spectrometry for high-resolution mass spectrometric analyses.

Contribution from the Department of Chemistry, Harvard University, Cambridge, Massachusetts 02138

The Cavitand Concept in the Synthesis of Subsite-Differentiated Analogues of Biological [4Fe-4S/Se]$^{2+}$ Clusters: Cluster Capture Reactions, Ligand Conformational Analysis, and the Structure of a Trigonal [4Fe-4Se]$^{2+}$ Analogue

T. D. P. Stack, J. A. Weigel, and R. H. Holm*

Received March 5, 1990

The previously reported clusters $[Fe_4S_4(Me_2LS_3)L']^{2-}$ (L' = RS^-, Cl^-) contain the cubane-type $[Fe_4S_4]^{2+}$ core and are derived from the trithiol $Me_2L(SH)_3$ (**1**, 1,3,5-tris((4,6-dimethyl-3-mercaptophenyl)thio)-2,4,6-tris(*p*-tolylthio)benzene), which as the trianion functions as a semirigid tridentate ligand. Iron sites are differentiated in the ratio 3:1. These clusters are analogous to certain biological clusters that undergo regiospecific reactions at the differentiated Fe site. In this work, the factors that render this unique ligand effective in cluster capture are explored. The reaction $[Fe_4Se_4(SEt)_4]^{2-}$ + **1** yields $[Fe_4Se_4(Me_2LS_3)(SEt)]^{2-}$; treatment of the latter cluster with 1 equiv of *t*-BuCOCl affords $[Fe_4Se_4(Me_2LS_3)Cl]^{2-}$ (**5**). $(Ph_4P)_2$[**5**]·2DMF crystallizes in the trigonal space group *P*3 with a = 24.733 (3) Å, c = 14.595 (3) Å, and Z = 3. The crystal structure consists of the three crystallographically independent clusters with imposed trigonal symmetry; these occur in a Δ:Λ ratio of 2:1 as refined crystallographically. The crystal is inversion-twinned, with only a slight preference for one enantiomer. The $[Fe_4Se_4]^{2+}$ core structures of the three clusters are nearly constant, but ligand conformations, described by tilt and cant angles of the coordinating arms of the ligand, are different. Formation of **5** reveals the flexibility of the ligand, inasmuch as the volume of the $[Fe_4Se_4]^{2+}$ core is 10% larger on the basis of atom coordinates and about 25% larger on the basis of van der Waals radii than that of the $[Fe_4S_4]^{2+}$ core. Cluster structures are analyzed in terms of ligand flexibility and conformation, cavity occupancy, and core structure. The clusters $[Fe_4S_4(Me_2LS_3)Cl)]^{2-}$ and $[Fe_4S_4(t\text{-}BuLS_3)Cl]^{2-}$ were isolated in high yield from the ligand-substitution reactions of **1** and *t*-BuL$(SH)_3$ (**2**, 1,3,5-tris((3-mercapto-5-*tert*-butylphenyl)thio)-2,4,6-tris(*p*-tolylthio)benzene), respectively, with $[Fe_4S_4(SEt)_4]^{2-}$ followed by reaction with pivaloyl chloride. In clear contrast, the related ligand $L(SH)_3$ (**3**), lacking the 4,6-dimethyl or 5-*t*-Bu substituents but otherwise identical, forms a mixture of soluble and polymeric clusters under the same conditions. ^{1}H NMR evidence is presented that the ligands exist in a solution conformation in which the three thiol-containing substituents (arms) are on one side of the central ring and the three *p*-tolylthio groups (legs) are on the other side. Because of the steric directing effects of the ring substituents on the arms of **1** and **2**, these molecules adopt dominant configurations with the three thiol groups turned inward over the central benzene ring. These configurations are recognized by the shielding of protons on the arms near the central ring. They are less populated with **3** because the molecule lacks the orienting effects of ring substituents. This situation is consistent with the results of a molecular dynamics analysis of **1** and **3**. Consequently, **1** and **2** are predisposed to capture a cubane-type cluster in ligand-substitution reactions and to suppress polymer formation. In this regard, these ligands may be considered to possess the principal attribute of cavitand molecules.

Introduction

Recently, we have summarized those structural and reactivity properties of the native cubane-type $Fe_4(\mu_3\text{-}S)_4$ clusters that are specific to a particular Fe subsite,[1-3] which is significantly differentiated by protein structure and environment from the other three subsites. The means of such differentiation are largely unknown and could involve terminal ligands other than cysteinyl thiolate and/or a coordination number exceeding 4. In the case of pig heart aconitase, it has now been established by protein crystallography that one subsite has a hydroxide or water terminal ligand and the other three subsites have conventional cysteinate ligation.[4]

In seeking synthetic analogues of such clusters, we have considered as a reasonable first step the synthesis of a tridentate trithiol ligand capable of spanning three of the subsites of a cluster and, ideally, affording a cluster species of overall trigonal symmetry. In this way, a 3:1 subsite population is created, affording the possibility of specific manipulation of the unique subsite. An approach such as this to analogue clusters is required inasmuch as the usual clusters $[Fe_4S_4(SR)_4]^{2-}$ of effectively cubic core symmetry undergo essentially statistical ligand substitution reactions.[3] Further, those anionic mixed ligand clusters that have been isolated[5] undergo statistical disproportionation in solution, and one cluster, $[Fe_4S_4(SC_6H_4\text{-}2\text{-}OH)_4]^{2-}$ as its Et_4N^+ salt, while crystallizing with one five-coordinate subsite, reverts to four-coordinate, equivalent subsites in solution.[6]

Tridentate ligands in the form of glycyl–cysteinyl oligopeptides have been shown to bind to clusters as products of substitution reactions with $[Fe_4S_4(S\text{-}t\text{-}Bu)_4]^{2-}$ in Me_2SO solution.[7] However,

(1) Stack, T. D. P.; Holm, R. H. *J. Am. Chem. Soc.* **1987**, *109*, 2546.
(2) Stack, T. D. P.; Holm, R. H. *J. Am. Chem. Soc.* **1988**, *110*, 2484.
(3) Holm, R. H.; Ciurli, S.; Weigel, J. A. *Prog. Inorg. Chem.*, in press.
(4) Robbins, A. H.; Stout, C. D. *Proc. Natl. Acad. Sci. U.S.A.* **1989**, *86*, 3639; *Proteins* **1989**, *5*, 289.
(5) (a) Kanatzidis, M. G.; Baenziger, N. C.; Coucouvanis, D.; Simopoulos, A.; Kostikas, A. *J. Am. Chem. Soc.* **1984**, *106*, 4500. (b) Kanatzidis, M. G.; Coucouvanis, D.; Simopoulos, A.; Kostikas, A.; Papaefthymiou, V. *J. Am. Chem. Soc.* **1985**, *107*, 4925.
(6) Johnson, R. E.; Papaefthymiou, G. C.; Frankel, R. B.; Holm, R. H. *J. Am. Chem. Soc.* **1983**, *105*, 7280.
(7) (a) Que, L., Jr.; Anglin, J. R.; Bobrik, M. A.; Davison, A.; Holm, R. H. *J. Am. Chem. Soc.* **1974**, *96*, 6042. (b) Burt, R. J.; Ridge, B.; Rydon, H. N. *J. Chem. Soc., Dalton Trans.* **1980**, 1228.

0020-1669/90/1329-3745$02.50/0

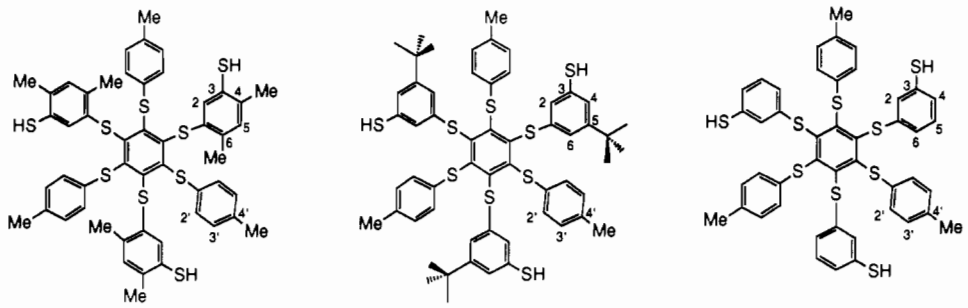

$Me_2L(SH)_3$ **1** **t-BuL$(SH)_3$** **2** **$L(SH)_3$** **3**

Figure 1. Formulas of the ligands $Me_2L(SH)_3$ (**1**), t-BuL$(SH)_3$ (**2**), and $L(SH)_3$ (**3**) and their atom-numbering schemes.

the ligands appear to lack the requisite rigidity to cause them to bind necessarily to a *single* cluster. NMR spectroscopy, the only feasible method to determine this structural aspect in solution, is indecisive in these cases.[7] Our initial approach to this problem, described at some length earlier,[2] has utilized as the tridentate ligand 1,3,5-tris((4,6-dimethyl-3-mercaptophenyl)thio)-2,4,6-tris(*p*-tolylthio)benzene, $Me_2L(SH)_3$[8] (**1**), shown in Figure 1. This compound has been synthesized in a convergent six-step scheme starting from 1,3,5-trifluorobenzene and *m*-xylene.[1,2] Its selection was predicted on the stereochemistry of $C_6(SPh)_6$[9] and related compounds[10,11] in which the substituent phenyl rings adopt alternate up–down conformations, designated ababab, with respect to the central benzene ring. If this conformation were to apply to a symmetrically substituted benzenetrithiol molecule, the coordinating "arms" would be disposed on the same side of the central ring. In this manner a cavity could be developed, not unlike those in the cavitands of Cram,[12] whose floor is the central benzene ring and whose "walls" are the closest edge regions of the rings of the three coordinating arms.

In reactions carried out thus far, ligand **1** behaves in the desired manner, binding a single Fe_4S_4 cluster at three Fe subsites and supporting fully regiospecific reactions with stoichiometric quantities of reagents at the unique subsite. In our earlier reports,[1,2] emphasis was placed on the structure and reactions of the clusters $[Fe_4S_4(Me_2LS_3)L']^{2-}$ ($L' = Cl^-, RS^-$). In subsequent work, we have shown that subsite-specific reactions may be used to place a large variety of mono-, bi-, and tridentate ligands at the unique subsite.[13] In this way, it has been possible to construct bridged double-cubane clusters[14] and to influence significantly redox potentials, electron distribution, and spin coupling among subsites.[15,16] With the efficacy of clusters derived from **1** now apparent, it is appropriate to investigate the factors that render this unique ligand effective as a tridentate sequestering agent of cubane-type clusters, including ligand flexibility and conformations, and other aspects of ligand design.

Experimental Section

Preparation of Compounds. Tridentate Ligands. (a) 1,3,5-Tris((4,6-dimethyl-3-mercaptophenyl)thio)-2,4,6-tris(*p*-tolylthio)benzene (1, $Me_2L(SH)_3$). The previously reported synthesis of this compound[2] has been altered in order to improve yields and significantly facilitate isolation of larger quantities of product. Changes in procedures are briefly summarized; spectroscopic and analytical data identifying the compounds have been given earlier.[2]

(i) 4,6-Dimethyl-3-((methoxymethyl)thio)benzenethiol. The preparation was based on 30.0 g (176 mmol) of 4,6-dimethylbenzene-1,3-dithiol.[17] Monodeprotection of 1,3-bis((methoxymethyl)thio)-4,6-dimethylbenzene with NaSEt was conducted at 110 °C for 4 h under dynamic vacuum. After the previous workup (excluding the silica plug filtration), the crude product was distilled rapidly (115 °C/0.10 Torr) to give 31.3 g of a clear viscous liquid. Column chromatography (63–200 mesh silica, 1:3 toluene/hexanes (v/v)) and rapid distillation gave 24.2 g of monoprotected dithiol; another 5.4 g of pure product was obtained by chromatography of mixed fractions and distillation for a 78% overall yield.

(ii) 1,3,5-Tris((4,6-dimethyl-3-((methoxymethyl)thio)phenyl)thio)-2,4,6-tris(*p*-tolylthio)benzene (1p). The preparation was run on a scale of 25 mmol of 1,3,5-trifluoro-2,4,6-tris(*p*-tolylthio)benzene[2] and 112 mmol of 4,6-dimethyl-3-((methoxymethyl)thio)benzenethiol in 100 mL of 3% H_2O/DMEU (1,3-dimethyl-2-imidazolidinone) (v/v). The reaction mixture was stirred for 3 days at room temperature and then for 2 days at 40 °C. Ether was added, and the reaction mixture was poured into 2 M HOAc. The organic layer was separated, washed with 5% NaOH (multiple times, to remove unreacted thiol) and saturated NaCl solution, and dried (Na_2SO_4). The crystalline product (contaminated with a minor impurity) was obtaied in >85% yield by recrystallization from hot acetone of the yellow residue after ether removal. Multiple recrystallizations from hot acetone (without cooling the solutions below room temperature) afforded 14.4 g (54%) of pure product. The solid material from the pooled filtrates was chromatographed (silica/toluene). Recrystallization of the solid from solvent removal of appropriate fractions increased the yield of pure product to 85%.

(iii) Formation of the Trithiol. A solution of the protected trithiol (8.0 g, 7.4 mmol) in 400 mL of chloroform and 20 mL of ethanol was thoroughly degassed. The following procedure was performed under a dinitrogen atmosphere. Solid $Hg(OAc)_2$ (7.8 g, 24.4 mmol) was added in one portion, and the mixture was stirred for a minimum of 12 h. After passage of H_2S for 20 min, the black mixture was filtered and the black residue was washed with hot chloroform until the washings were colorless. Solvent from the combined filtrate and washings was removed to give a yellow residue, which was washed with hot acetonitrile and dried in vacuo, affording 6.80 g (97%) of pure trithiol **1**.

(b) 1,3,5-Tris((3-mercapto-5-*tert*-butylphenyl)thio)-2,4,6-tris(*p*-tolylthio)benzene (t-BuL$(SH)_3$, 2). (i) 3,5-Dibromo-*tert*-butylbenzene. 3,5-Dibromo-*tert*-butylbenzene was prepared from *tert*-butylbenzene by a sequence of standard reactions: mononitration[18] (80%), reduction over Raney nickel[19] (93%), dibromination with bromine[20] (57%), and reduc-

(8) In our other papers on this subject, this compound has been abbreviated as $L(SH)_3$, a designation now used for the compound with no alkyl substituents on the mercaptophenyl ring. The introduction of substituents in this work requires that they be identified in the compound designation.
(9) (a) MacNicol, D. D.; Hardy, A. D. U.; Wilson, D. R. *Nature* **1977**, *266*, 611. (b) Hardy, A. D. U.; MacNicol, D. D.; Wilson, D. R. *J. Chem. Soc., Perkin Trans. 2* **1979**, 1011.
(10) Gilmore, C. J.; MacNicol, D. D.; Murphy, A.; Russell, M. A. *Tetrahedron Lett.* **1983**, 3269.
(11) MacNicol, D. D. In *Inclusion Compounds*; Atwood, J. L., Davies, J. E. D., MacNicol, D. D., Eds.; Academic Press: New York, 1984; Vol. 2, Chapter 5.
(12) (a) Morgan, J. R.; Karbach, S.; Cram, D. J. *J. Am. Chem. Soc.* **1982**, *104*, 5826. (b) Cram, D. J. *Science* **1983**, *219*, 1177. (c) Cram, D. J. *Angew. Chem., Int. Ed. Engl.* **1988**, *27*, 1009.
(13) Weigel, J. A.; Holm, R. H. Results to be published.
(14) Stack, T. D. P.; Carney, M. J.; Holm, R. H. *J. Am. Chem. Soc.* **1989**, *111*, 1670.
(15) Ciurli, S.; Carrié, M.; Weigel, J. A.; Carney, M. J.; Stack, T. D. P.; Papaefthymiou, G. C.; Holm, R. H. *J. Am. Chem. Soc.* **1990**, *112*, 2654.
(16) Weigel, J. A.; Holm, R. H.; Surerus, K. K.; Münck, E. *J. Am. Chem. Soc.* **1989**, *111*, 9246.
(17) (a) Morgenstern, J.; Mayer, R. *Z. Chem.* **1968**, *8*, 106. (b) Wagner, A. W. *Chem. Ber.* **1966**, *99*, 375.
(18) Nelson, K. L.; Brown, H. C. *J. Am. Chem. Soc.* **1951**, *73*, 5605.
(19) Biekart, H. J. B.; Dessens, H. B.; Verkade, P. E.; Wepster, B. M. *Recl. Trav. Chim. Pays-Bas* **1952**, *71*, 321.

tive deamination with *tert*-butyl nitrite[21] (65%). The compound was obtained as a white crystalline solid after recrystallization from 95% ethanol; mp 31–32 °C. ^{1}H NMR ($CDCl_3$): δ 1.29 (9), 7.43 (2), 7.48 (1).

(ii) 3,5-Dimercapto-*tert*-butylbenzene. The method of Testaferri et al.[22] was employed. To a stirred slurry of 32.0 g (327 mmol) of sodium isopropylthiolate in 600 mL of *N*,*N*-dimethylacetamide (DMA) was added 19.1 g (65.3 mmol) of 3,5-dibromo-*tert*-butylbenzene. This mixture was heated to 100 °C, 10.5 g (457 mmol) of sodium (small pieces) was added slowly after 24 h, and the mixture was maintained at 100 °C for another 24 h, cooled to ambient temperature, and poured into 3 L of 0.1 M HCl. Acidification (3 M HCl), extraction into ether, drying of extracts (Na_2SO_4), and solvent removal in vacuo gave 13.9 g of crude red oil. The material in dichloromethane was passed through a silica plug. Solvent was removed, affording a yellow oil, vacuum distillation of which yielded 9.7 g (74%) of product as a light yellow oil. ^{1}H NMR ($CDCl_3$): δ 1.27 (9), 3.42 (2), 7.03 (1), 7.07 (2).

(iii) 3-((Methoxymethyl)thio)-5-*tert*-butylphenyl Thioacetate. 3-((Methoxymethyl)thio)-5-*tert*-butylbenzenethiol was prepared by the method for 4,6-dimethyl-3-((methoxymethyl)thio)benzenethiol[2] on a 36% scale. The crude product (7.6 g) as a red oil was esterified with 1.1 equiv of acetyl chloride in dichloromethane (2 equiv of pyridine, 0.02 equiv of 4-(dimethylamino)pyridine as catalyst) to give 8.1 g of a red oil. Column chromatography (multiple passes) of this oil on flash silica afforded 2.76 g (34%) of product as a viscous light yellow oil. ^{1}H NMR ($CDCl_3$): δ 1.31 (9), 2.41 (3, MeCO), 3.43 (3, OMe), 4.97 (2, CH_2); 7.28, 7.36 (1,1; 4-H, 6-H); 7.50 (1, 2-H).

(iv) 1,3,5-Tris((3-((methoxymethyl)thio)-5-*tert*-butylphenyl)thio)-2,4,6-tris(*p*-tolylthio)benzene (2p). Sodium (0.143 g, 6.20 mmol) was added to 20 mL of dry methanol. After dihydrogen evolution subsided, 1.79 g (6.25 mmol) of the acetate in 5 mL of methanol was added and the solution was stirred overnight. The solvent was removed in vacuo, and the gummy residue was washed with ether, leaving a white powder. This material was dissolved in 20 mL of 3% water/DMEU (v/v). Addition of 0.520 g (1.04 mmol) of 1,3,5-trifluoro-2,4,6-tris(*p*-tolylthio)-benzene[2] caused an immediate color change to dark yellow. The reaction mixture was stirred for 3 days at room temperature, causing a color change to red-orange. The mixture was poured onto ether and extracted with saturated $NaHCO_3$ and water, and the organic layer was dried (Na_2SO_4). Solvent removal in vacuo gave 1.20 g of a yellow oil. Gradient flash chromatography using mixtures of toluene and hexanes yielded 0.88 g (73%) of pure product as a yellow solid, mp 100–105 °C. ^{1}H NMR ($CDCl_3$): δ 1.20 (9, *t*-Bu), 2.24 (3, 4′-Me), 3.36 (3, OMe), 4.84 (2, CH_2); 6.82, 6.90 (1,1, d, 2′-H, 3′-H); 6.85 (1, 2-H), 6.87 (1, 6-H); 7.17 (1, 4-H). ^{13}C NMR ($CDCl_3$): δ 149.3, 152.3 (central ring).

(v) Formation of the Trithiol. The protected trithiol was fully deprotected by the method for **1** and was obtained in 95% yield as a yellow solid, mp >200 °C (diffuse). ^{1}H NMR ($CDCl_3$): δ 1.17 (9, *t*-Bu), 2.24 (3, 4′-Me), 3.33 (1, SH), 6.47 (1, 2-H); 6.80, 6.93 (1,1; d, 2′-H, 3′-H); 6.87, 6.97 (1,1; 4-H, 6-H). ^{13}C NMR ($CDCl_3$): 149.6, 152.5 (central ring). FAB-MS (3-nitrobenzyl alcohol; *m*/*e* (M^+)): calcd 1032.2181; obsd 1032.2196.

(c) 1,3,5-Tris((3-mercaptophenyl)thio)-2,4,6-tris(*p*-tolylthio)benzene (3). (i) 3-((Methoxymethyl)thio)benzenethiol. This compound was prepared from 1,3-dimercaptobenzene[22,23] by using the method for the 4,6-dimethyl derivative. During purification, the compound was distilled at 128 °C (0.05 Torr). The pure product was obtained as a colorless oil. ^{1}H NMR ($CDCl_3$): δ 3.43 (3, Me), 4.95 (2, CH_2), 7.15 (1, s, 5-H); 7.12, 7.24 (1, 1; d/t, 4-H, 6-H); 7.39 (1, t, 2-H). FAB-MS (neat; *m*/*e*): 186 (M^+).

(ii) 1,3,5-Tris((3-((methoxymethyl)thio)phenyl)thio)-2,4,6-tris(*p*-tolylthio)benzene (3p). The preparation followed that for the 4,6-dimethyl derivative but with use of 3-((methoxymethyl)thio)benzenethiol. The product was purified by gradient flash column chromatography (100/0% to 97/3% (v/v) toluene/ethyl acetate). Multiple passes were required to purify the product, which was obtained as a gummy yellow solid in 40% yield. During purification, slow degradation on silica was observed. No suitable solvent for recrystallization was found. ^{1}H NMR ($CDCl_3$): δ 2.27 (3, Me), 3.38 (3, OMe), 4.90 (2, CH_2), 6.74 (1, d, 6-H); 6.86, 6.96 (1, 1; d, 2′-H, 3′-H); 7.06 (1, s, 2-H), 7.08 (1, t, 5-H), 7.18 (1, d, 4-H). ^{13}C NMR ($CDCl_3$): δ 146.3, 149.4 (central ring). FAB-MS (3-nitrobenzyl alcohol; *m*/*e*): 996 (M^+). Anal. Calcd for $C_{51}H_{48}O_3S_9$: C, 61.41; H, 4.85. Found: C, 60.97; H, 4.52.

(iii) Formation of the Trithiol. The trithiol **3** was obtained in nearly quantitative yield as a yellow gummy material by deprotection of the foregoing compound in a manner entirely analogous to that used in the synthesis of **1**.[2] The purification method for **1** (which is nearly insoluble in acetonitrile) was inapplicable owing to the appreciable solubility of the product in acetonitrile. The trithiol as isolated was used in subsequent experiments. ^{1}H NMR ($CDCl_3$): δ 2.27 (3, Me), 6.70 (1, d, 6-H), 6.73 (1, s, 2-H); 6.87, 6.95 (1, 1; d, 2′-H, 3′-H); 6.97 (1, d, 4-H), 7.03 (1, t, 5-H). FAB-MS (3-nitrobenzyl alcohol; *m*/*e*): 864 (M^+).

Hexakis((3-((methoxymethyl)thio)phenyl)thio)benzene (9p). This compound was prepared in a manner similar to that for other hexakis-(phenylthio)benzenes[2] except that C_6F_6 and 9.0 equiv of the sodium thiolate were employed. The product was purified by gradient flash chromatography. The crude material was loaded on the column with toluene, and the percentage of ethyl acetate in the eluting solvent was slowly increased to a final composition of 90:10 toluene/ethyl acetate (v/v). Two passes were necessary to purify the material, which was obtained in 55% yield. ^{1}H NMR ($CDCl_3$): δ 3.37 (3, OMe), 4.89 (2, s, CH_2), 6.72 (1, d, 6-H), 7.08 (1, t, 5-H), 7.10 (1, s, 2-H), 7.18 (1, d, 4-H). ^{13}C NMR ($CDCl_3$): δ 148.3 (central ring). FAB-MS (3-nitrobenzyl alcohol; *m*/*e*): 1182 (M^+). Anal. Calcd for $C_{54}H_{54}O_6S_{12}$: C, 54.79; H, 4.60. Found: C, 54.65; H, 4.40.

Hexakis((3-mercaptophenyl)thio)benzene (9). Deprotection of the previous compound was similar to that described for the preparation of **1**. ^{1}H NMR ($CDCl_3$): δ 3.43 (1, s, SH), 6.74 (1, d, 6-H), 6.80 (1, s, 2-H), 7.01 (1, d, 4-H), 7.07 (1, t, 5-H). ^{13}C NMR ($CDCl_3$): δ 147.9 (central ring). FAB-MS (3-nitrobenzyl alcohol; *m*/*e*): 918 (M^+).

Clusters. All operations were performed under a pure dinitrogen atmosphere; solvents were thoroughly degassed prior to use.

(a) $(Ph_4P)_2[Fe_4S_4(Me_2LS_3)Cl]$ (4). The following is a simpler and higher yield preparation than the original.[2] Compound **1** (3.50 g, 3.69 mmol) was dissolved in 250 mL of refluxing chloroform. To the cooled solution was added 4.71 g (3.69 mmol) of $(Ph_4P)_2[Fe_4S_4(SEt)_4]$[24] in 30 mL of DMF. The reaction mixture was stirred under dynamic vacuum for 1 h, and the remaining chloroform was removed in vacuo with gentle heating. Pivaloyl chloride (0.49 g, 1.1 equiv) was added, and the reaction mixture was stirred for 30 min and filtered. Acetonitrile (300 mL) was added to the filtrate, and the solution was stored at −20 °C. Collection of separated solid by filtration followed by washing with cold acetonitrile and drying in vacuo gave 6.10 g (82%) of pure product as black microcrystals. An additional 0.50 g was recovered from the filtrate by solvent removal and recrystallization (DMF/acetonitrile), for a total yield of 88%. Properties of the compound are given elsewhere.[2]

(b) $(Ph_4P)_2[Fe_4Se_4(Me_2LS_3)Cl]$ (5). The preceding method was followed with use of 0.53 mmol of **1** and $(Ph_4P)_2[Fe_4Se_4(SEt)_4]$.[25] After reaction with pivaloyl chloride, the solution was filtered and an equal volume of ether added to the filtrate. Black hexagonal blocks formed overnight. These were collected, washed with ether, and dried under vacuum to give 0.94 g (81%) of product. The compound was not analyzed but was unambiguously identified as the pure cluster product by spectroscopic, electrochemical, and crystallographic properties. Absorption spectrum (DMF), λ_{max} (ϵ_M): 480–490 nm (sh, 10000). ^{1}H NMR (Me_2SO-d_6): δ 2.17 (3, 4′-Me), 4.04 (3, 6-Me), 4.28 (3, 4-Me), 5.02 (1, 2-H), 6.50 (1, 3′-H), 7.01 (1, 2′-H), 8.48 (1, 5-H). $E_{1/2}$ (ΔE_p) (DMF): −0.95 V (2−/3−, vs SCE) (90 mV). The compound is only sparingly soluble in acetonitrile.

(c) $(Ph_4P)_2[Fe_4S_4(t\text{-}BuLS_3)Cl]$ (6). This compound was prepared in a dichloromethane/acetonitrile solvent by using the procedure for **4**. Solvent removal afforded a black solid, which, because of its very high solubility, could not be crystallized. However, physical properties identified the compound, and it was found to be pure by ^{1}H NMR spectroscopy. Absorption spectrum (DMF), λ_{max} (ϵ_M): 450 (sh, 10300) nm. ^{1}H NMR (CD_3CN): δ 1.27 (9, *t*-Bu), 2.25 (3, 4′-Me), 4.55 (1, 2-H), 5.13 (1, 4-H), 6.08 (1, 6-H), 6.70 (2, 3′-H), 7.11 (2, 2′-H). $E_{1/2}$ (ΔE_p) (DMF): −1.01 V (2−/3−, vs SCE) (95 mV).

Collection and Reduction of X-ray Data. Suitable crystals of compound **5** as hexagonal blocks were obtained by vapor diffusion of ether into a DMF solution. The ^{1}H NMR spectrum of these crystals indicated the presence of DMF solvate. To minimize solvent loss, the crystals were mounted directly in glass capillaries after removing the recrystallization solvent and washing with ether. Diffraction data were collected at room temperature on a Nicolet P3F four-circle automated diffractometer with

(20) Schaefer, T.; Kruczynski, L. J.; Krawchuk, B.; Sebastian, R.; Charlton, J. L.; McKinnon, D. M. *Can. J. Chem.* **1980**, *58*, 2452.
(21) Doyle, M. P.; Dellaria, J. F.; Siegfried, B.; Bishop, S. W. *J. Org. Chem.* **1977**, *42*, 3494.
(22) Testaferri, L.; Tiecco, M.; Tingoli, M.; Chianelli, D.; Montanucci, M. *Synthesis* **1983**, 751.
(23) Vögtle, R.; Lichtenhaler, R. G.; Zuber, M. *Chem. Ber.* **1973**, *106*, 719.
(24) Averill, B. A.; Herskovitz, T.; Holm, R. H.; Ibers, J .A. *J. Am. Chem. Soc.* **1973**, *95*, 3523.
(25) This compound was prepared according to the procedure for other $[Fe_4Se_4(SR)_4]^{2-}$ clusters: Bobrik, M. A.; Laskowski, E. J.; Johnson, R. W.; Gillum, W. O.; Berg, J. M.; Hodgson, K. O.; Holm, R. H. *Inorg. Chem.* **1978**, *17*, 1402.

Table I. Crystallographic Data for $(Ph_4P)_2[Fe_4Se_4(Me_2LS_3)Cl]\cdot 2DMF$

formula	$C_{105}H_{99}ClFe_4N_2O_2P_2S_9Se_4$
fw	2346.2
a, Å	24.733 (3)
c, Å	14.595 (3)
Z	3
V, Å^3	7732 (2)
space group	P3
d_{calc} (d_{obs}), g/cm^3	1.50 (1.51)
μ, cm^{-1}	22.3
$R(F_o)$, %	5.20 (5.29)[a]
$R_w(F_o^2)$, %	5.50 (5.58)[a]

[a] Other enantiomer.

use of graphite-monochromatized Mo Kα radiation. Unit cell parameters and orientation matrices were obtained for 25 strong, machine-centered reflections ($20° \le 2\theta \le 25°$). Crystallographic data are set out in Table I. Three check reflections monitored every 123 reflections exhibited no significant decay over the course of the data collection. Lorentz and polarization corrections were applied with the program XTAPE of the SHELXTL program package (Nicolet XRD Corp., Madison, WI). An empirical absorption correction, PSICOR, was judged necessary and applied. The lack of mirror symmetry in axial photographs in conjunction with the lack of systematic absences in the 000l reflections indicated a trigonal cell and space group $P3$ (No. 143) or $P\bar{3}$ (No. 147). Density measurements indicated $Z = 3$ for the unit cell with five or six molecules of DMF. Space group $P\bar{3}$ was rejected because of the inability of the proposed structure of **5** to reside on an inversion center as would be required for $Z = 3$. The simple E statistics from MULTAN supported the choice of a noncentrosymmetric space group, which was confirmed by successful refinement of the structure.

Solution and Refinement of the Structure. Atom scattering factors were taken from the tabulations of Cromer and Waber.[26] At a minimum, the atoms of the Fe_4Se_4 core were located by direct methods (MULTAN 80) using random groups that were constructed in the program CHEMX from appropriate crystal structures. Three independent thirds of a cluster anion were found, requiring that each such anion be trigonally symmetric: one Se, one Fe, and the Cl atom of each independent anion (Fe(x1), Se(x1), Cl(x1); x = 1–3) must reside on one of three unique 3-fold axes. All remaining non-hydrogen atoms except for two carbon atoms of solvate molecules were located by use of Fourier maps. Two least-squares refinements were required to locate these atoms. Atom Cl(11) was taken as the point of origin to fix the z coordinate. The structure was refined by using CRYSTALS, with phenyl rings treated as semirigid bodies using the method of additional observational equations[27] except for the central ring (ring 0). The solvate molecules were loosely constrained by similar means. Isotropic refinement converged at R = 8.8%. In further refinements, all non-hydrogen molecules were anisotropically refined except for those of the solvate molecules. Hydrogen atoms were included at 0.96 Å from all anisotropically refined atoms, with isotropic thermal parameters 1.2× those of the bonded atom. The final difference map exhibited two peaks of ca. 0.6 e/Å^3 in the vicinity of the Fe(22,32) atoms. All other peaks were <0.5 e/Å^3. Final R values are given in Table I. The refinement of the enantiomorph generated by inverting the coordinates through the origin indicated that the original coordinate set was slightly favored. Convergence of the polarity factor[28] to 0.05 (2) in further refinements with the original coordinate set suggested that the crystal was inversion-twinned. Refinement of the crystal data as an inversion twin gave a value of 0.475 (13) for the absolute structure factor.[29] This value indicates that the slightly preferred enantiomorph comprises ≈52% of the macroscopic sample while the remaining volume, ≈48%, is filled by the inverse enantiomorph. The relatively small esd of the absolute structure factor indicates that the anomalous scattering was significant in the structure factor calculations. Positional parameters of the preferred enantiomorph are listed in Table II.[30] All calculations and discussions will concern only this enantiomorph.

Other Physical Measurements. Spectrophotometric, spectroscopic, and electrochemical measurements were performed under anaerobic conditions where appropriate by using the equipment and procedures described earlier.[2]

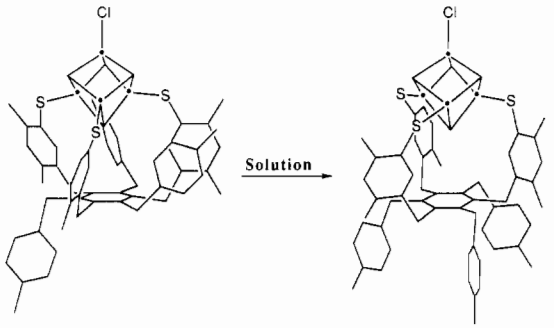

aaabaa ababab (C_3)

Figure 2. Depictions of the aaabaa structure of $[Fe_4S_4(Me_2LS_3)Cl]^{2-}$ (**4**) as its Ph_4P^+ salt in the solid state and the trigonally symmetric (ababab) conformation of $[Fe_4S_4(Me_2LS_3)L]^{2-}$ (L = Cl$^-$, RS$^-$) in solution.[2]

Results and Discussion

The compounds **1**–**9** specified below (**p** = protected thiol) are of principal interest to the results and considerations that follow.

$Me_2L(SR)_3$	R = H	**1**	R = CH_2OMe	**1p**
t-BuL$(SR)_3$	R = H	**2**	R = CH_2OMe	**2p**
$L(SR)_3$	R = H	**3**	R = CH_2OMe	**3p**
$[Fe_4S_4(Me_2LS_3)Cl]^{2-}$		**4**		
$[Fe_4Se_4(Me_2LS_3)Cl]^{2-}$		**5**		
$[Fe_4S_4(t\text{-}BuLS_3)Cl]^{2-}$		**6**		
$C_6(SPh)_6$		**7**		
$C_6(SC_6H_4\text{-}6\text{-}Me)_6$		**8**		
$C_6(SC_6H_4\text{-}3\text{-}SR)_6$	R = H	**9**	R = CH_2OMe	**9p**

The structures of tridentate ligands **1**–**3** are provided in Figure 1. The synthesis of ligand **1** has been very considerably improved in terms of simplified procedures and yield compared to the original report.[2] Ligands **2** and **3** have not been previously reported. Molecular conformations of these ligands are described at two levels. In the first, the a/b nomenclature[31] for substituents above (a) and below (b) the plane of the central benzene ring (ring 0) specifies the gross conformation. A more precise description is afforded by the tilt (θ) and cant (ϕ) angles for each substituent. These are defined by the dihedral angles formed by the shaded atoms in **10** and **11** relative to a planar reference configuration with $\theta = \phi = 0°$; this method of conformational analysis is described fully elsewhere.[2]

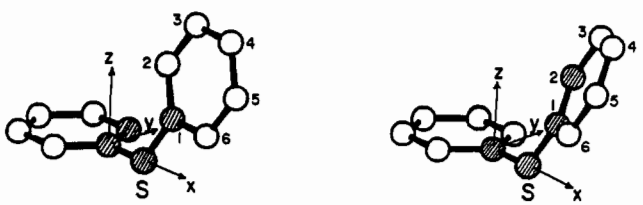

10 (θ) **11** (ϕ)

We have previously described the binding function of **1** as that of a semirigid tridentate ligand with dimensions suitable for attaching an Fe_4S_4 cluster at three Fe subsites.[2] As shown in Figure 2, cluster **4** as its crystalline Ph_4P^+ salt displays the desired tridentate coordination mode to a single cluster, with the ligand in the aaabaa conformation. The three coordinating "arms" are on the same side of the ligand, whereas two of the "legs" are on this side and one is on the opposite side. In DMF-d_7 solution down to 220 K, the isotropically shifted ^{1}H NMR spectra are consistent with the trigonally symmetric conformation ababab, indicative of a ligand conformation change upon passing from the crystalline to the solution state.

Here we probe more closely the structural aspects of ligand **1**

(26) Cromer, D. T.; Waber, J. T. *International Tables for X-ray Crystallography*; Kynoch Press: Birmingham, England, 1974; Vol. IV.
(27) Waser, J. *Acta Crystallogr.* **1962**, *16*, 1091.
(28) Rodgers, D. *Acta Crystallogr.* **1981**, *A37*, 734.
(29) (a) Bernadelli, G.; Flack, H. D. *Acta Crystallogr.* **1985**, *A41*, 500. (b) Flack, H. D. *Acta Crystallogr.* **1983**, *A39*, 876.
(30) See paragraph at the end of this article concerning supplementary material.
(31) MacNicol, D. D.; Mallinson, P. R.; Robertson, C. D. *J. Chem. Soc., Chem. Commun.* **1985**, 1649.

Table II. Positional Parameters ($\times 10^4$) for $[Fe_4Se_4(Me_2LS_3)Cl]^{2-}$

atom	x/a	y/b	z/c	atom	x/a	y/b	z/c
			Core and Ligands for Structure A				
Fe(12)	734 (1)	534 (1)	3092 (2)	C(116)	2010 (4)	2297 (4)	6016 (6)
Se(12)	268 (1)	1004 (1)	2171 (1)	C(117)	2644 (5)	2563 (6)	3578 (7)
Cl(11)	0	0	0	C(118)	2109 (6)	2691 (7)	6854 (8)
Fe(11)	0	0	1537 (2)	C(101)	545 (6)	581 (6)	6840 (7)
Se(11)	0	0	4309 (2)	C(102)	−47 (7)	544 (7)	6836 (8)
S(111)	1208 (2)	1332 (2)	7057 (3)	C(121)	120 (4)	1565 (5)	7842 (7)
S(121)	−114 (3)	1221 (2)	6752 (3)	C(122)	313 (4)	2193 (5)	7888 (7)
S(112)	1759 (2)	1153 (2)	3419 (3)	C(123)	484 (4)	2503 (5)	8723 (8)
C(111)	1584 (4)	1659 (4)	6011 (6)	C(124)	472 (4)	2201 (5)	9522 (7)
C(112)	1500 (4)	1309 (4)	5213 (6)	C(125)	275 (4)	1569 (5)	9472 (7)
C(113)	1839 (4)	1597 (4)	4423 (6)	C(126)	94 (4)	1253 (5)	8645 (6)
C(114)	2266 (4)	2238 (4)	4424 (6)	C(127)	656 (4)	2545 (7)	10422 (9)
C(115)	2343 (4)	2576 (5)	5220 (7)				
			Core and Ligands for Structure B				
Fe(22)	−2696 (1)	−6688 (1)	−2941 (2)	C(216)	−1009 (4)	−5747 (4)	152 (6)
Se(22)	−2422 (1)	−5786 (1)	−3885 (1)	C(217)	−601 (7)	−5619 (7)	−2369 (9)
Cl(21)	−3333	−6667	−6039 (4)	C(218)	−673 (6)	−5393 (5)	993 (8)
Fe(21)	−3333	−6667	−4536 (2)	C(201)	−2744 (5)	−6616 (6)	1094 (7)
Se(21)	−3333	−6667	−1706 (2)	C(202)	−2794 (5)	−6066 (5)	1094 (7)
S(211)	−1999 (2)	−6565 (2)	1212 (2)	C(221)	−2022 (4)	−4976 (5)	2071 (7)
S(221)	−2108 (2)	−5330 (2)	1008 (3)	C(222)	−1858 (4)	−4350 (5)	2118 (7)
S(212)	−1911 (2)	−6841 (2)	−2495 (3)	C(223)	−1727 (4)	−4038 (5)	2959 (8)
C(211)	−1611 (4)	−6260 (4)	166 (6)	C(224)	−1763 (4)	−4352 (6)	3765 (7)
C(212)	−1881 (4)	−6560 (4)	−652 (6)	C(225)	−1931 (4)	−4980 (5)	3717 (8)
C(213)	−1567 (5)	−6369 (5)	−1486 (7)	C(226)	−2053 (4)	−5284 (5)	2875 (7)
C(214)	−964 (4)	−5854 (4)	−1492 (7)	C(227)	−1625 (4)	−4010 (8)	4658 (9)
C(215)	−699 (5)	−5554 (5)	−676 (7)				
			Core and Ligands for Structure C				
Fe(32)	3571 (1)	7413 (1)	−10504 (2)	C(316)	3161 (4)	8745 (4)	−13439 (6)
Se(32)	2638 (1)	6991 (1)	−9578 (1)	C(317)	3552 (5)	9386 (5)	−11021 (9)
Cl(31)	3333	6667	−7431 (4)	C(318)	2873 (4)	8849 (5)	−14283 (8)
Fe(31)	3333	6667	−8944 (2)	C(301)	3287 (8)	7204 (7)	−14241 (8)
Se(31)	3333	6667	−11722 (2)	C(302)	3875 (7)	7249 (6)	−14241 (8)
S(311)	3236 (2)	7889 (2)	−14475 (3)	C(321)	4938 (5)	8078 (4)	−15254 (7)
S(321)	4557 (2)	8001 (2)	−14191 (3)	C(322)	4611 (5)	7796 (4)	−16052 (7)
S(312)	4017 (2)	8440 (2)	−10844 (3)	C(323)	4934 (5)	7872 (4)	−16863 (7)
C(311)	3350 (4)	8301 (4)	−13424 (7)	C(324)	5581 (5)	8234 (4)	−16898 (6)
C(312)	3599 (4)	8201 (4)	−12633 (6)	C(325)	5897 (5)	8516 (4)	−16094 (8)
C(313)	3676 (4)	8547 (4)	−11840 (6)	C(326)	5584 (6)	8444 (5)	−15271 (8)
C(314)	3498 (4)	8999 (4)	−11850 (6)	C(327)	5937 (7)	8326 (5)	−17772 (8)
C(315)	3242 (4)	9087 (4)	−12646 (6)				

[a] Labeling scheme for the three independent anions:

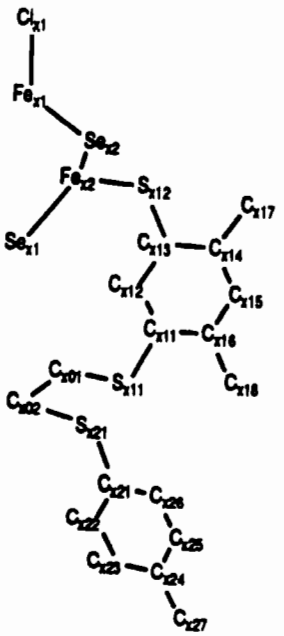

that allows for effective cluster capture. We first explore the flexibility of the ligand, in terms of its ability to bind cores larger than $[Fe_4S_4]^{2+}$, and then investigate the effect of ring substituents on the arms in predisposing the ligand toward binding of a single cluster.

Flexibility. The most easily accessible test of the flexibility of **1** is made with $[Fe_4Se_4]^{2+}$ clusters, a number of which have been prepared earlier.[25,32-36] The core volume is substantially larger

Table III. Selected Interatomic Distances (Å) and Angles (deg) for $[Fe_4Se_4(Me_2LS_3)Cl]^{2-}$ [a,b]

	$x = 1$	$x = 2$	$x = 3$
	Cluster[c]		
Fe(x1)–Cl(x1)	2.243 (3)	2.194 (7)	2.209 (6)
Fe(x1)–Se(x2)	2.413 (3)	2.412 (3)	2.415 (3)
Fe(x2)–Se(x2)	2.414 (3)	2.413 (3)	2.416 (3)
Fe(x2)–Se(x1)	2.408 (3)	2.412 (3)	2.413 (3)
Fe(x2)–Se(x2′)	2.400	2.415	2.412
mean	2.409 (6)	2.413 (1)	2.414 (2)
Fe(x2)–S(x12)	2.261 (4)	2.252 (4)	2.262 (4)
Fe(x1)–Fe(x2)	2.792 (3)	2.826 (3)	2.801 (3)
Fe(x2)–Fe(x2′)	2.817	2.776	2.827
Fe(x1)–Se(x1)	4.046 (4)	4.130 (3)	4.054 (4)
Fe(x2)–Se(x2′)	4.082	4.060	4.093
Se(x1)–Se(x2)	3.835 (2)	3.877 (2)	3.844 (2)
Se(x2)–Se(x2′)	3.859	3.839	3.865
Cl(x1)–Fe(x1)–Se(x2)	112.56 (7)	113.20 (7)	112.50 (8)
Se(x2)–Fe(x1)–Se(x2′)	106.22	105.50	106.29
Se(x1)–Fe(x2)–Se(x2)	105.35 (8)	106.93 (8)	105.48 (9)
Se(x1)–Fe(x2)–Se(x2′)	105.79	106.84	105.60
Se(x2)–Fe(x2)–Se(x2′)	106.58	105.36	106.33
Fe(x1)–Se(x2)–Fe(x2)	70.70 (8)	71.71 (7)	70.87 (8)
Fe(x1)–Se(x2)–Fe(x2′)	70.93	71.67	70.93
Fe(x1)–Se(x1)–Fe(x2′)	71.58	70.25	71.70
Fe(x2)–Se(x2)–Fe(x2′)	71.62	70.19	71.67
S(x12)–Fe(x2)–Se(x1)	119.9 (1)	114.6 (1)	119.5 (1)
S(x12)–Fe(x2)–Se(x2)	115.8 (1)	116.9 (1)	115.5 (1)
Fe(x2)–S(x12)–C(x13)	119.4 (3)	107.1 (3)	110.4 (3)
	Ligand		
S(x11)–C(x11)	1.759 (9)	1.760 (10)	1.784 (10)
S(x11)–C(x01)	1.786 (13)	1.792 (11)	1.793 (14)
S(x21)–C(x02)	1.766 (14)	1.767 (12)	1.780 (13)
S(x21)–C(x21)	1.759 (11)	1.741 (11)	1.775 (10)
S(x12)–C(x13)	1.782 (10)	1.807 (11)	1.766 (10)
C(x01)–S(x11)–C(x11)	108.9 (5)	105.5 (5)	108.1 (5)
C(x21)–S(x21)–C(x02)	103.5 (5)	105.6 (5)	104.6 (6)
ring 0 centroid to Se(x1)	3.690	4.086	3.676
ring 0 mean plane to S(x12)	4.989	5.238	4.958
(ring 0 centroid)–C(x13)–S(x12)	106.52	112.51	106.61
dev from ring 0 mean plane[d]			
C(x01)	−0.003	0.000	+0.001
C(x02)	+0.003	0.000	−0.001
S(x11)	−0.320	−0.173	−0.341
S(x21)	+0.125	+0.125	+0.073
core vol, Å^3	10.68	10.68	10.78

[a] Symmetry-related atoms are primed. [b] Nonunique distances were calculated by CHEMX. [c] $x = 1$ (**5A**), $x = 2$ (**5B**), $x = 3$ (**5C**). [d] Positive displacements are toward the cluster.

in selenide clusters, the increase being 10.4% for $[Fe_4Q_4(SPh)_4]^{2-}$ [25,37] and 10.3% for $[Fe_4Q_4Cl_4]^{2-}$ [35,38] (Q = S, Se). Such increases result nearly entirely from increases in the volumes of the Q_4 tetrahedra as opposed to the Fe_4 tetrahedra.[39] These volumes and those in Table III were calculated from atom coordinates; they present the volume of the core based on nuclear positions. This method provides a consistent means of comparing cubane-type clusters of different sizes. However, a proper conception of the accommodation of a cubane-type unit in **1** requires an estimate of the difference in van der Waals volume of $[Fe_4Se_4]^{2+}$ vs $[Fe_4S_4]^{2+}$.

$[Fe_4S_4(Me_2LS_3)Cl]^{2-}$

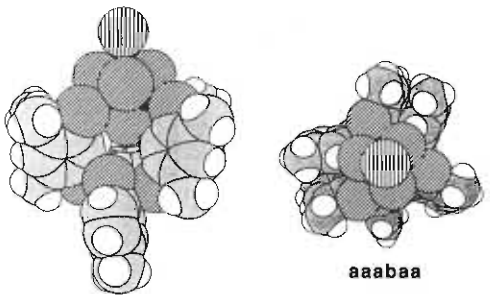

$[Fe_4Se_4(Me_2LS_3)Cl]^{2-}$

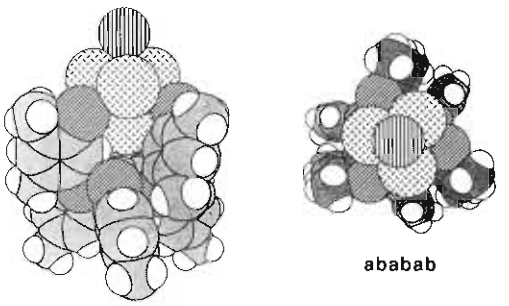

Figure 3. Space-filling models of $[Fe_4S_4(Me_2LS_3)Cl]^{2-}$ (**4**) and $[Fe_4Se_4(Me_2LS_3)Cl]^{2-}$ (**5A**) viewed parallel (left) and perpendicular (right) to the 3-fold axis. The four Se atoms eclipse the Fe atoms; the hydrogen atoms visible near the lower (unique) chalcogenide atom in the parallel views are 2-H.

Numerical integration of the cubane cores using the program OPEC[40] with appropriate radii[41] consistently gives a 25% larger volume for the selenium-containing cores: $[Fe_4S_4(SPh)_4]^{2-}$ (87.6 Å^3) vs $[Fe_4Se_4(SPh)_4]^{2-}$ (109.6 Å^3), 25.1%; **4** (87.9 Å^3) vs **5A** (110.1 Å^3), 25.3%. This increase in volume is almost completely accounted for in the Q-atom region. An examination of cluster insertion into **1** with space-filling models, shown in Figure 3, reveals that the volume increase can be readily accommodated in the three Q = S, Se sites directly bonded to the unique Fe atom. Note that the three Q atoms are positioned slightly above the clefts formed by the three upwardly projected arms. The remaining Q atom in each structure is located *within* the cavity. Accommodation of a 25% volume increase in this unique atom will severely restrict the tilt and cant values of the arms through nonbonded interactions (vide infra).

$[Fe_4Se_4(Me_2LS_3)Cl]^{2-}$. (a) Preparation. Cluster **5** was prepared by reaction 1, analogous to the method for **4**. The initial mo-

$$[Fe_4Se_4(SEt)_4]^{2-} + Me_2L(SH)_3 \rightarrow [Fe_4Se_4(Me_2LS_3)(SEt)]^{2-} + 3EtSH \xrightarrow{t\text{-BuCOCl}} [Fe_4Se_4(Me_2LS_3)Cl]^{2-} + t\text{-BuCOSEt} \quad (1)$$

(32) Christou, G.; Ridge, B.; Rydon, H. N. *J. Chem. Soc., Dalton Trans.* **1978**, 1423.
(33) Reynolds, J. G.; Coyle, C. L.; Holm, R. H. *J. Am. Chem. Soc.* **1980**, *102*, 4350.
(34) (a) Moulis, J.-M.; Meyer, J. *Biochemistry* **1982**, *21*, 4762. (b) Moulis, J.-M.; Meyer, J.; Lutz, M. *Biochemistry* **1984**, *23*, 6605.
(35) Wei, C.; Liu, H. *Jiegou Huaxue (J. Struct. Chem.)* **1986**, *5*, 203.
(36) Rutchik, S.; Kim, S.; Walters, M. A. *Inorg. Chem.* **1988**, *27*, 1513.
(37) Que, L., Jr.; Bobrik, M. A.; Ibers, J. A.; Holm, R. H. *J. Am. Chem. Soc.* **1974**, *96*, 4168.
(38) Bobrik, M. A.; Hodgson, K. O.; Holm, R. H. *Inorg. Chem.* **1977**, *16*, 1851.
(39) A thorough study of this point has been made by Henkel and coworkers: Simon, W., Thesis, Universität Münster, 1988. Henkel, G. Private communication. For example, across the series $[Fe_4Q_4(SPh)_4]^{2-}$ (Q = S, Se, Te), $V(Fe_4)$ increased by 8.7% whereas $V(Q_4)$ increased by 58%, leading to a volume enlargement of $[Fe_4Q_4]^{2+}$ by 23%.
(40) Gavezzotti, A. *J. Am. Chem. Soc.* **1985**, *107*, 962.
(41) Shannon, R. D. *Acta Crystallogr.* **1976**, *A32*, 751. The radii used were 0.70 Å (high-spin $Fe^{2+,3+}$), 1.70 Å (S^{2-}), and 1.84 Å (Se^{2-}). The above core volume increases are practically the same as the volume increase of selenide over sulfide (26.8%), indicating that the overlap of the Q_4 tetrahedron with the Fe_4 tetrahedron in both cluster pairs is nearly equivalent and that the Q atoms do not significantly overlap with each other.

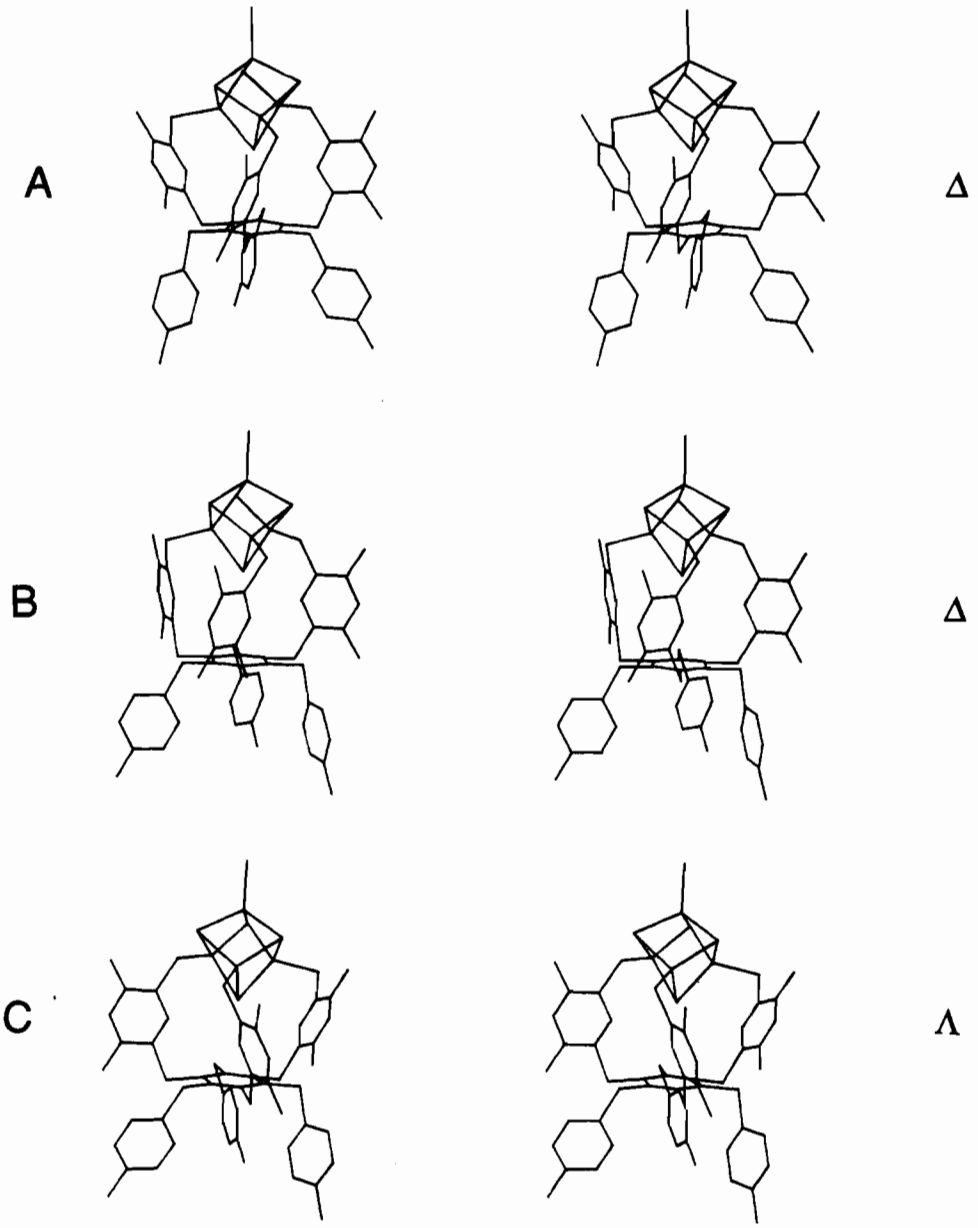

Figure 4. Stereoviews of the three independent anions **5A**, **5B**, and **5C** of $[Fe_4Se_4(Me_2LS_3)Cl]^{2-}$. The chirality of each is given.

noethanethiolate cluster was generated under dynamic vacuum (to remove ethanethiol) in $CHCl_3$/DMF and was not isolated. After removal of the chloroform, it was converted in situ to the monochloro species in a site-specific reaction with a 10% excess of pivaloyl chloride. The cluster was isolated in 81% yield as its Ph_4P^+ salt.

The compound crystallizes as $(Ph_4P)_2[Fe_4Se_4(Me_2LS_3)Cl]\cdot 2DMF$ from DMF/ether in the trigonal system with the uncommon space group $P3$.[42] The crystal structure consists of discrete anions, cations, and solvate molecules. The asymmetric unit contains two cations, two solvate molecules, and three independent thirds of an anion, each of which resides on one of the three 3-fold axes. Stereoviews of symmetry-generated independent anions **5A–C** appear in Figure 4, the corresponding cluster portions of the structures are provided in Figure 5, and two views of the unit cell packing are set out in Figure 6, from which the beautiful packing scheme is evident. Each cluster is coordinated in the mode for which ligand **1** was designed. Selected interatomic distances and angles are collected in Table III; the anion-labeling scheme is presented at the end of Table II. Note the relationship between cluster designations **5A–C** and the atom-numbering scheme (Table III, footnote *c*). The structures of the anions are analyzed in terms of conformations, core units, and cavity occupancy.

(b) Conformations. Each of the three independent clusters in the unit cell has trigonal symmetry, with the 3-fold axes parallel to the *c* axis of the unit cell and containing the atoms Cl(x1)–Fe(x1)–Se(x1) (x = 1–3). The conformations are abababab, in contrast to the solid-state structure of **4** (Figure 1). The interaction of the cubane core and the ligand renders each cluster anion chiral and is conveyed by the sign of the dihedral angle Fe(x1)–Fe(x2)–S(x12)–C(x13). Clusters **5A** and **5B** have positive angles of 151.5 and 149.3°, respectively, while that of cluster **5C** is 151.1° and opposite in sign.[43] When viewed down the 3-fold Cl(x1)–Fe(x1) axis, positive and negative values of this angle relate to the Δ (**12**) and Λ (**13**) absolute configurations, respectively.[44] The axes of clusters **5A** and **5B** point in the negative *c* direction, while

(42) The space group has occurred in only 23 out of 71 860 crystal structures: Cambridge Structural Data Base, University Chemical Laboratories, Cambridge, U.K.

(43) These angles are defined under the Klyne–Prelog sign convention: when one is looking from atom B to atom C in the generalized torsional angle A–B–C–D, the clockwise rotation of A to obtain superposition is positive.

(44) These designations correspond to IUPAC chirality nomenclature; cf., e.g.: Thewalt, U.; Jensen, K. A.; Schäffer, C. E. *Inorg. Chem.* **1972**, *11*, 2129.

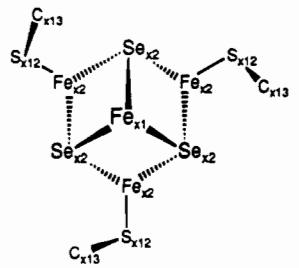

12 (Δ)

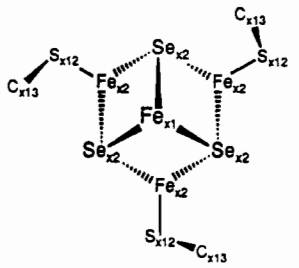

13 (Λ)

that of cluster **5C** is in the positive c direction. The pairing of configurations is the same as the directionality of the 3-fold axes. The compound has undergone spontaneous partial resolution within the unit cell in an enantiomeric ratio of 2:1 as refined crystallographically. Attempts to define the absolute chirality through the significant anomalous dispersion of the crystal indicated that, in fact, the crystal was inversion-twinned with only a slight preference for one enantiomorph. In order to facilitate discussion of cluster structures, the slightly preferred enantiomorph will be analyzed.

Conformational angles (θ, ϕ) for the three independent clusters **5** and for the sulfido cluster **4** are given in Table IV. The absolute configurations are best appreciated by consideration of cluster racemization, which is summarized in reaction 2. It can be

$$(\theta, \phi) \rightleftharpoons (180 - \theta, -\phi) \qquad (2)$$

conceptualized as a trigonal twist about the C_3 axis, which in the $\Delta \rightarrow \Lambda$ conversion, for example, requires a clockwise rotation. During this process, the cluster rises above the floor of the cavity to a maximum height when the C(x02)–C(x01)–S(x11)–S(x21) dihedral angle is +90°. Such a conformation corresponds to the achiral transition state. Cluster **5B** most closely approaches this state. Continued twisting in the same sense recovers the enantiomer. The ligand/cluster dynamic interaction is very much analogous to a mechanical device with limited degrees of freedom; the arms move in unison with the twisting. A clockwise rotation to move the cluster into the cavity gives the Λ isomer while the opposite rotation gives the Δ isomer.

(c) Core Units. The imposed trigonal symmetry requires that the six faces of each $[Fe_4Se_4]^{2+}$ core divide into two sets of three that contain either Fe(x1) or Se(x1) and reduces to three the number of unique Fe–Se distances. A fourth Fe–Se distance is generated by symmetry-related atoms. Other sets of independent distances and angles are readily obtained from Table III. Compared to those in $[Fe_4Se_4L_4]^{2-}$ (L = PhS^-,[25] Cl^-,[35] Br^-[36]), Fe–Se, Fe–Fe, and other distances and angles are not exceptional, and core volumes are nearly constant. Indeed, the variance in Fe–Se distances is small; such distances fall into the narrow range 2.400 (3)–2.416 (3) Å. The Fe–Cl bond lengths are variable, with that in cluster **5A** (2.243 (2) Å) being ca. 0.02 Å longer than any other such bond. Core volumes are somewhat larger than that of $[Fe_4Se_4(SPh)_4]^{2-}$ (10.54 Å^3) and close to that of $[Fe_4Se_4Cl_4]^{2-}$ (10.70 Å^3).

The most significant feature of each core is its trigonal distortion. The nonbonded distances Fe(x1)–Se(x1) and Fe(x2)–Se(x2′) (Table III) measure the height (h) and width (w), respectively, of the core. From the indicated h:w ratios, clusters **5A** and **5C** (both 0.991) are trigonally compressed and cluster **5B** (1.02) is trigonally elongated. The larger volume of the core of **5C** vs **5A** follows from the slightly larger h and w values. This classification of distortion is consistent with S(x12)–S(x12′) separations, which are largest for cluster **5B**.

(d) Cavity Occupancy. Relevant metric data are contained in Table III. The positioning of the cores in the ligand cavity and the accompanying adjustments of ligand structural features are coactions with core distortion. The most incisive parameter that differentiates cavity occupancy is the distance from the centroid of ring 0 to Se(x1). For trigonally compressed clusters **5A** and **5C**, these separations are 3.690 and 3.676 Å, respectively, near the van der Waals radius contact distance of 3.54 Å[41,45] between the ring and a selenium atom. Connecting atoms S(x11) are substantially displaced below the plane of ring 0 (−0.320 Å for x = 1 and −0.341 Å for x = 3). With reference to the atom numbering scheme (Figure 7 or 8), we observe that the distances between the inwardly projected 2-H atoms of the arms and the unique Se atom (Se(x1), 2.87 Å in **5A** and 2.88 Å in **5C**), are essentially at the estimated minimum van der Waals distance of 2.84 Å. (The position of one 2-H atom in cluster **5A** can be seen in Figure 3.) We conclude that in **5A** and **5C** the core approaches or achieves full occupancy of the ligand cavity.

In comparison, for the trigonally elongated cluster **5B**, the distance from the ring 0 centroid to Se(21) is 4.086 Å and the displacement of S(211) is only −0.173 Å. The distance between the 2-H atom and Se(21) is 3.24 Å. Further, the terminal sulfur atom S(212) is 0.26 Å farther above ring 0 than are the S(x12) atoms (x = 1, 3). These factors reflect the higher position of the core in its cavity, thus filling it to a lesser extent than is the case for clusters **5A** and **5C**. The fuller occupancies of the cavities of the latter two clusters is apparently not compatible with trigonal elongation. Indeed, it is likely that the relatively small Fe(12)–Se(11) and Fe(12)–Se(12′) bond lengths (2.408 and 2.400 Å, respectively) arises from a van der Waals interaction between ring 0 and Se(11) in cluster **5A**.

Crystalline compound **5** displays several features that have not been encountered previously. It is the first cluster complex of ligand **1** with the ababab conformation and provides the first instance, in any environment, of a trigonally distorted $[Fe_4X_4]^{2+}$ core.[46] More important for present purposes, however, is the finding that a cubane-type core unit of the size of $[Fe_4Se_4]^{2+}$, as well as the smaller $[Fe_4S_4]^{2+}$, can be accommodated in a 3:1 subsite-differentiated binding mode by cavitand ligand **1**. Moreover, this ligand and $[Fe_4Se_4]^{2+}$ acting in synergy have found three solutions for cavity occupancy.

Precise comparisons between the sulfide and selenide cluster structures are hampered by differences in ligand conformations. Yet some trends can be observed. In all four structures, ligand **1** interacts with the cores in a chiral sense such that *all* arms within a cluster have tilt angles whose θ − 90° values are either *all* positive or negative, thus assuring near-trigonal coordination symmetry. The relationships between tilt, cant, and Fe–Fe–C–S dihedral angles are shown in Table V. The sign of neither the tilt angle nor cant angle correlates with chirality over the four structures available. Note that a correlation of the sign of the cant angle with chirality applies to **5A–C** but is not maintained in **4**. This situation can be understood with reference to Figure 7. Here, projections of the C(2)–H(2) bond vectors on the plane of the central benzene ring convey chirality. The directional sense of the vector sets for the two Δ configurations (**5A**,**B**) is opposite that of the Λ configuration. This correlation is a manifestation of the increased volume included in the ligand cavities of these clusters. The magnitudes of the cant angles of **5A–C** is considerably larger than those of **4** (mean 7.45°, Table IV). The nonbonded interactions of the three 2-H atoms with the unique Se atom, as described above, cause an outward canting of the arms in order to minimize these interactions. Similar interactions in **4** are less severe, the mean 2-H···S distance being 2.89 Å and the van der Waals contact distance being 2.70 Å. This allows a greater flexibility in the choice of cant angles.

It is evident from the structures of four clusters now available that the semirigid nature of ligand **1** permits flexibilities in several structural aspects sufficient to bind the $[Fe_4S_4]^{2+}$ and $[Fe_4Se_4]^{2+}$ cores. Further, the cubane-type cores $[VFe_3S_4]^{2+}$ and $[MoFe_3S_4]^{3+}$ have also been inserted into the ligand by binding at the three Fe sites.[47]

(45) Huheey, J. E. *Inorganic Chemistry*, 3rd ed.; Harper & Row: New York, 1983; Chapter 6.

(46) The large majority of $[Fe_4X_4L_4]^{2-}$ clusters, with unidentate terminal ligands, have tetragonally distorted core units: (a) Berg, J. M.; Holm, R. H. In *Metal Ions in Biology*; Spiro, T. G., Ed.; Interscience: New York, 1982; Vol. 4, Chapter 1. (b) Carney, M. J.; Papaefthymiou, G. C.; Spartalian, K.; Frankel, R. B.; Holm, R. H. *J. Am. Chem. Soc.* **1988**, *110*, 6084 and references therein.

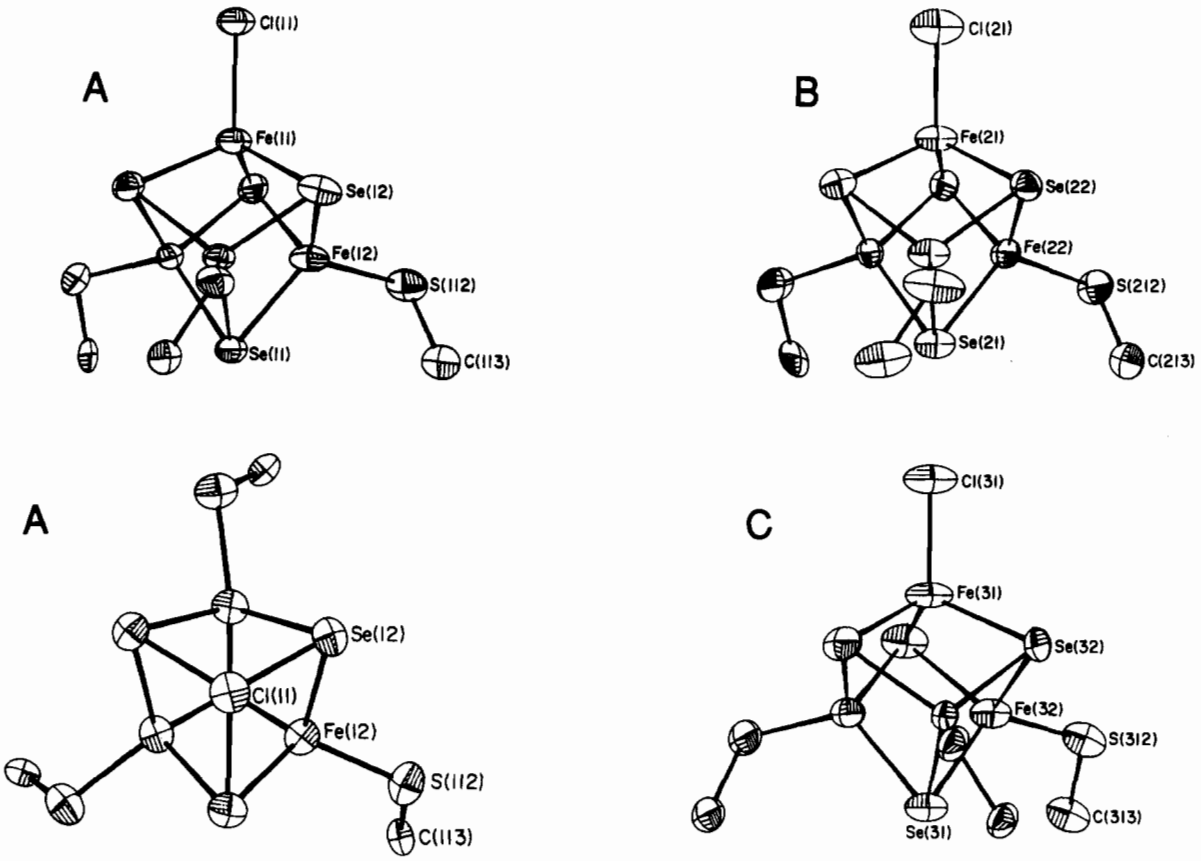

Figure 5. Structures of the cluster portions of the three independent anions of $[Fe_4Se_4(Me_2LS_3)Cl]^{2-}$ showing atom-numbering schemes and 50% probability ellipsoids. The structure at the lower left is a view down the 3-fold axis (coincident with the Cl(11)–Fe(11) bond) of anion **5A**, displaying the imposed trigonal symmetry. The primed atoms in Table III are related to the labeled atoms under this symmetry.

Table IV. Conformational Analysis of Clusters

conformation	angle	tilt and cant angles for arm/leg,[a] deg 1[b]	2	3	4	5	6	ref
			$[Fe_4S_4(Me_2LS_3)Cl]^{2-}$					
aaabaa	θ	86.20	45.02	78.51	−75.37	77.76	52.52	2
	ϕ	−12.49	53.98	0.04	−12.10	9.84	46.98	
			$[Fe_4Se_4(Me_2LS_3)Cl]^{2-}$[c]					
5A, Δ, ababab	θ	89.30	−73.60					*d*
	ϕ	−19.08	−24.25					
5B, Δ, ababab	θ	114.30	−111.04					*d*
	ϕ	−56.59	50.09					
5C, Λ, ababab	θ	106.37	−115.12					*d*
	ϕ	15.83	30.95					

[a] The 1,3,5-substituents are arms; the 2,4,6-substituents are legs. [b] Carbon atom numbering scheme follows the designation of crystallographic coordinates. [c] Imposed C_3 symmetry. [d] This work.

Table V. Relationship of the Signs of Tilt (**10**), Cant (**11**), and Fe–Fe–S–C (**12**/**13**) Angles and the Absolute Configurations of Clusters **4** and **5A–C**

cluster	sign $\theta - 90°$	sign ϕ	Fe(x1)–Fe(x2)–S(x12)–C(x13), deg	chirality
4[a]	−	−	+157.4	
	−	+	+155.1	Δ
	−	+	+146.8	
5A[b]	−	−	+151.5	Δ
5B[b]	+	−	+149.7	Δ
5C[b]	+	+	−151.1	Λ

[a] The Ph_4P^+ salt crystallizes in point group $P\bar{1}$; both enantiomers are present in the unit cell. [b] Imposed trigonal symmetry.

Solution Conformation of $[Fe_4Se_4(Me_2LS_3)Cl]^{2-}$. Solution spectroscopic results indicate that the $[Fe_4Se_4]^{2+}$ core is comfortably accommodated in ligand **1** in a manner very similar to **4**. The ^1H NMR spectrum of cluster **5**, shown in Figure 8, is entirely analogous to that of **4** in acetonitrile,[2] but with slightly larger isotropic shifts. The same effect occurs in the spectra of other $[Fe_4Q_4(SR)_4]^{2-}$ clusters and arises from the larger paramagnetism of the Q = Se cluster.[25] The spectrum is consistent with trigonal symmetry, strongly suggesting that the ababab conformation in the solid state is retained in solution. As shown in Figure 2, **4** also adopts this conformation in solution, necessitating a change from the solid-state structure.[2]

Ligand Design. Having established that **1**, *once bound*, functions as a flexible tridentate ligand capable of accommodating cubane-type cores of different sizes, we next consider those aspects that allow it to bind these cores efficiently. Our original conception of an appropriate tridentate ligand for site differentiation included a substituent of sufficient size at the 5- or 6-position of the coordinating arm. This was thought to cause an orientation of each arm such that the 3-SH group would be projected preferentially inward over the central ring, thus providing a prepared confor-

(47) Ciurli, S.; Holm, R. H. *Inorg. Chem.* **1989**, *28*, 1685.

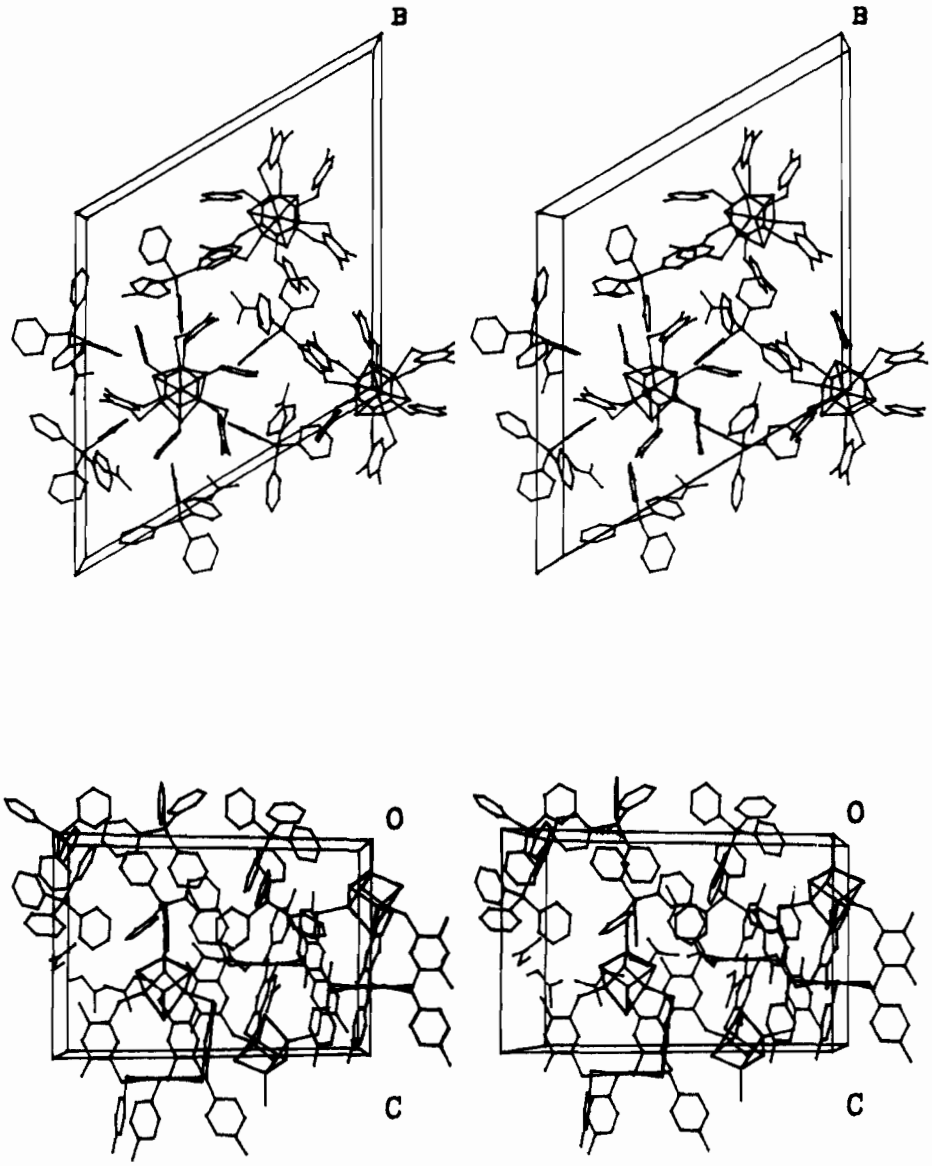

Figure 6. Packing diagrams of $(Ph_4P)_2[Fe_4Se_4(Me_2LS_3)Cl]\cdot 2DMF$. Top: view down the *a* axis showing the orientation of the clusters in the unit cell. Bottom: view showing 3-fold axes parallel to the *c* axis.

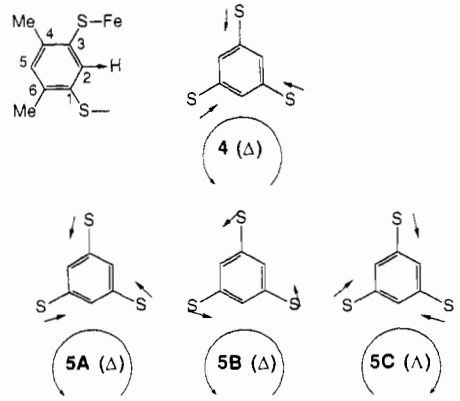

Figure 7. Projection of C(2)–H(2) bond vectors on the plane of the central benzene ring in clusters **4** and **5A–C**. Sulfur atoms of the ligand arms are shown. In **5A–C**, the vector sets correlate with chirality, whereas this relationship is not maintained for **4**.

mation for cluster capture. We investigate this matter here by use of ligands **2** and **3** (Figure 1), which were synthesized in a manner similar to that for **1**.[2]

From reactions completely analogous to reaction 1, we have isolated chloro clusters **4** and **6** in yields exceeding 80%. The ^1H NMR spectrum of **6**, which was derived from **2**, is shown in Figure 9 and is entirely consistent with trigonal symmetry. The spectrum of **4**, which has the same property, was given earlier.[2] The behavior of ligand **3** was very different. Reaction of equimolar $[Fe_4S_4(SEt)_4]^{2-}$ and **3** in chloroform/acetonitrile followed by standard workup afforded a black solid that, when isolated, was only partially soluble in Me_2SO. The ^1H NMR spectrum of the soluble portion was indicative of a mixture of paramagnetic products, as indicated by multiple signals in the 8 ppm (5-H, Figure 8) and 5–6 ppm (4-H, 6-H, Figure 9) regions. Elsewhere, we have shown that the chemical shifts of these protons (particularly 5-H) are extremely sensitive to ligation at other Fe subsites.[2,13–15] We conclude that ligand **3**, which lacks any orienting substituents, forms a mixture of products that are predominantly oligomeric in nature. In a clear contrast, ligands **1** and **2** form monocluster products in high isolated yields. This difference in reactivity would appear to be attributable to a structural predisposition of **1** and **2** favorable for cluster binding. This matter has been investigated by an analysis of shielding effects on ^1H NMR chemical shifts and by molecular dynamics calculations.

Free Ligand Conformations. (a) Proton Shielding. In solution, all hexakis(arylthio)benzenes prepared in this and earlier work[2] display ^1H and ^{13}C NMR spectra at and below ambient temperature that are entirely consistent with effective trigonal symmetry. The molecules in question either exist in one stable conformation of the appropriate symmetry or are mixtures of nearly isoenergetic, rapidly interconverting conformers whose chemical

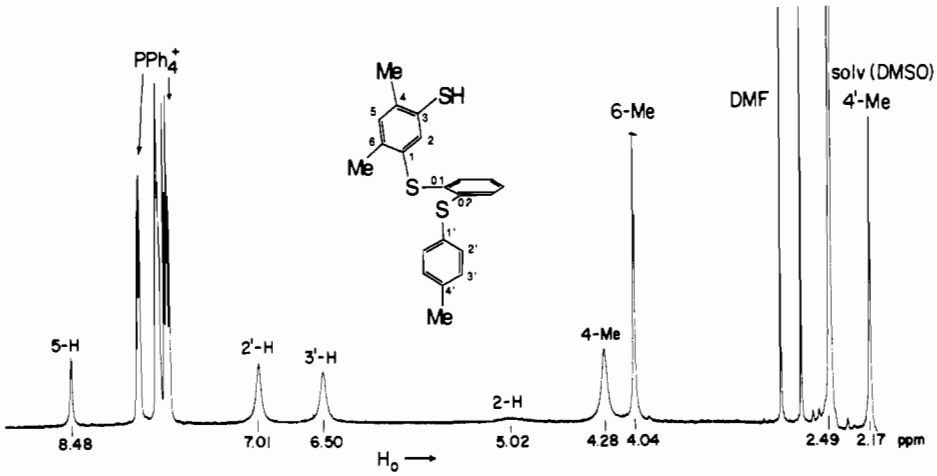

Figure 8. ^{1}H NMR spectrum of $[Fe_4Se_4(Me_2LS_3)Cl]^{2-}$ (**5**) in Me_2SO-d_6 at 297 K. The ligand numbering scheme is shown and signal assignments are indicated.

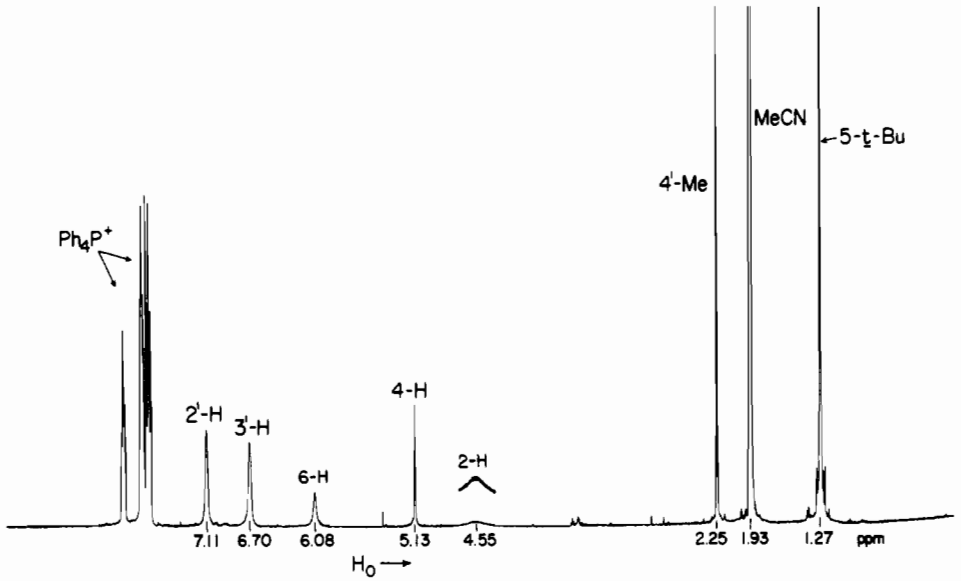

Figure 9. ^{1}H NMR spectrum of $[Fe_4S_4(t\text{-}BuLS_3)Cl]^{2-}$ (**6**) in CD_3CN at 297 K. The ligand numbering scheme is that in Figure 1; signal assignments are indicated.

Table VI. Minimized Energies (kcal/mol) for $C_6(SPh)_6$ (**7**)

con-formation	energy					
	total	bond	angle	torsional	VDW	electrostatic
aaaaaa	46.1	8.0	1.2	1.2	37.2	−1.5
aaaaab	46.9	7.8	0.7	0.4	38.4	−0.4
aaaabb	47.7	7.8	0.6	0.3	38.5	0.5
aaabbb	47.8	7.8	0.6	0.2	38.7	0.5
ababbb	47.6	7.6	0.3	0.03	39.3	0.4
abbabb	48.1	7.6	0.3	0.1	39.1	1.0
ababab	48.9	7.6	0.2	0.04	40.1	1.0
aabaab	49.3	7.6	0.6	0.1	39.5	1.5

shifts are averaged to apparent trigonal symmetry. We have extended previous measurements at 210 K to 185 K in CD_2Cl_2, as shown by the ^{1}H NMR spectra of compounds **7** and **8** in Figure 10 and find no evidence indicative of dynamic behavior for any compound.[48] As previously,[2] we consider the first explanation, implicating the ababab conformation, to be the more plausible.

Molecular mechanics calculations using the CHARMM force field (vide infra) indicate that the eight possible conformations of **7** are separated in energy by only 3.2 kcal/mol. Even though the

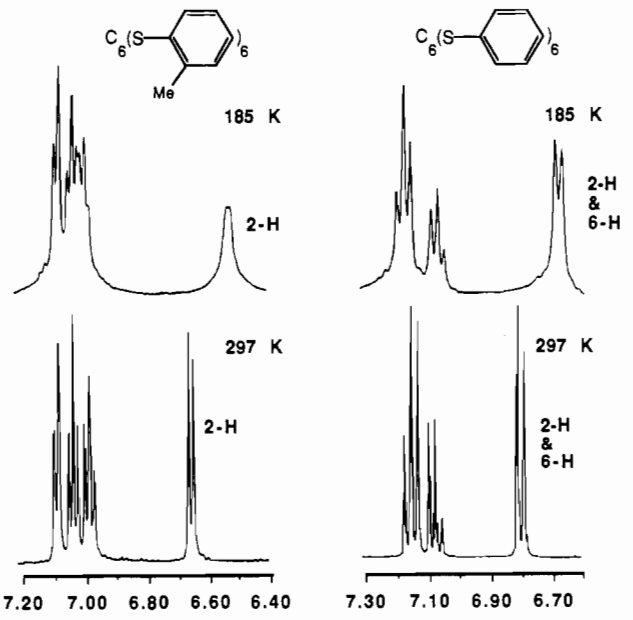

Figure 10. ^{1}H NMR spectra of **7** (right) and **8** (left) in CD_2Cl_2 solutions at 185 and 297 K illustrating the shielding of 2-H and 6-H (**7**) and 2-H (**8**).

(48) Peak broadening at 185 vs 297 K is most likely due to an increase in solvent viscosity.

Table VII. Shielding Effects on Ring Protons in Hexakis(arylthio)benzenes[a]

compound	ref[b]	$\lvert\delta_{ref} - \delta_{cpd}\rvert$, ppm						
		2-H	3-H	4-H	5-H	6-H	2′-H[c]	3′-H[c]
Ph_2S	A_1	−0.09	−0.02	−0.11	−0.02	−0.09		
7	A_1	0.32	0.13	0.03	0.13	0.32		
8[d]	A_2	0.55	0.19	0.04	0.10			
9	B_1	0.59		0.11	0.08	0.50		
9p	C_1	0.48		0.12	0.10	0.58		
3	B_1	0.66		0.14	0.12	0.54	0.32	0.15
3p	C_1	0.52		0.12	0.10	0.56	0.33	0.14
2	B_3	0.76		0.19		0.41	0.39	0.17
2p	C_3	0.57		0.15		0.45	0.37	0.20
1	B_2	1.01			0.15		0.33	0.11
1p	C_2	0.88			0.14		0.34	0.21

[a] All spectra were taken in $CDCl_3$ solution at 297 K. [b] Reference compounds:

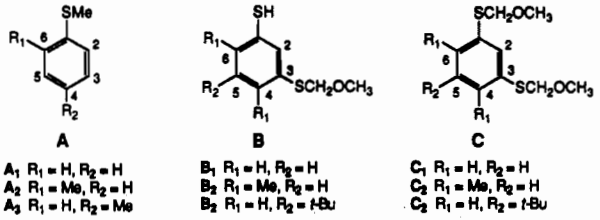

[c] The reference compound for these protons is A_3. [d] For the purpose of comparison, the numbering scheme has been altered (2-Me to 6-Me) so that protons correspond with those in the rest of the table.

energy-minimized ababab conformation has the most favorable bond and angle contributions, the aaaaaa ("all-up") conformation is the most stable. Minimized energies are listed in Table VI together with individual contributions.[49] Relative to ababab, stabilization of the aaaaaa conformation derives from the favorably attractive van der Waals (VDW) and electrostatic energies that arise from the more compact arrangement of substituents. Flexible molecules tend to minimize their energies by folding up in a vacuum. Geometrical considerations dictate that the all-up conformation is particularly well suited to promote these two energy contributions; all phenyl substituents can reside above the central ring without significant bond/angle distortions and VDW repulsions while allowing the electrostatically favorable edge-to-face ("herringbone") packing of rings.[50] Once in solution, it is probable that the importance of these self-complementary stabilization energies will be minimized and the conformations with lesser bond angle and bond distance distortions will be favored.

A limitation of the CHARMM force field in the present cases is the lack of inclusion of lone pairs on the sulfur atoms. Ab initio calculations indicate that explicit inclusion of lone pairs on sulfur is required for adequate parameterization.[51] Because these atoms are in close contact (as is evident from the large VDW energies), the lone-pair/lone-pair interactions will play an important role in determining the lowest energy conformation. A related situation is found with hexaethylbenzene, where adjacent CH_2/CH_2 interactions determine the energy ordering of the eight conformations.[52] Calculations using the MM2 force field with lone pairs on the sulfur atoms of $C_6(SMe)_6$ (a model for molecules with larger substituents) indicate that the ababab conformation is the most stable, and the aaaaaa conformation the least stable, by 3.6 kcal/mol. These molecular mechanics studies suggest that in solution the ababab conformation should predominate but that other conformations could be populated at room temperature. Hereafter, we take this to be the major conformation in solution.

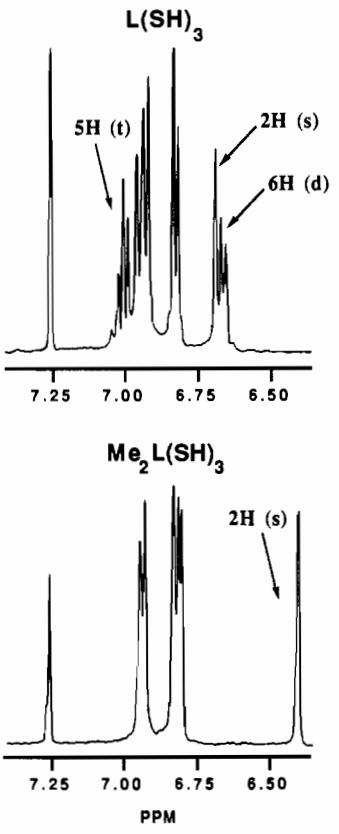

Figure 11. ^1H NMR spectra of ligands **3** (top) and **1** (bottom), in $CDCl_3$ solutions at 297 K illustrating the shielding of 2-H (**1**) and 2,6-H (**3**).

A conspicuous feature of the ^1H NMR spectra of all hexakis(arylthio)benzene molecules, which is evident in the spectra of **7** and **8** in Figure 10 and of ligands **1** and **3** in Figure 11, is the significant shielding of the 2-H and 6-H atoms of the central ring substituents. In the case of **1** in $CDCl_3$, the 2-H resonance, which appears at 6.45 ppm at 297 K, is shifted upfield by 0.24 ppm at 223 K; all other shifts change by ≤0.04 ppm. This indicates an increased population of configurations that effect shielding of 2-H. Diphenyl sulfide, the basic subunit of hexakis(arylthio)benzene molecules, lacks this shielding effect. A tabulation of shielding effects is presented in Table VII.[53] These

(49) The energy minimum searches were restricted to initial configurations as symmetric as possible and were generally limited to 10 different initial configurations.
(50) Burley, S. K.; Petsko, G. A. *Science* **1985**, *229*, 23; *J. Am. Chem. Soc.* **1986**, *108*, 7995.
(51) (a) Singh, U. C.; Kollman, P. C. *J. Comput. Chem.* **1984**, *5*, 129. (b) Weiner, S. J.; Kollman, P. C.; Case, D. A.; Singh, U. C.; Ghio, C.; Alagona, G.; Profeta, S., Jr.; Weiner, P. *J. Am. Chem. Soc.* **1984**, *106*, 765.
(52) Iverson, D. J.; Hunter, G.; Blount, J. F.; Damewood, J. R., Jr.; Mislow, K. *J. Am. Chem. Soc.* **1981**, *103*, 6073.

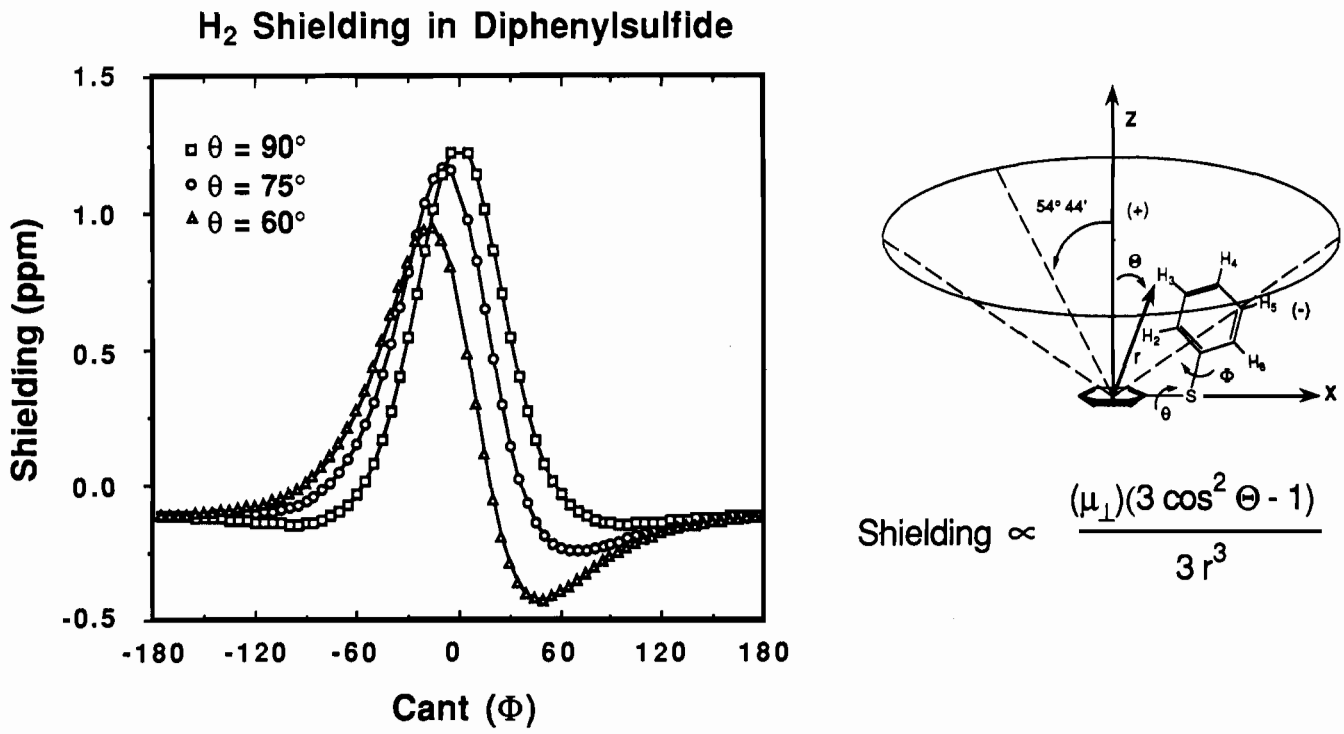

Figure 12. Shielding of 2-H in one ring by the other ring as dependent on the tilt and cant angles (θ, ϕ) of diphenyl sulfide. The shielding values were calculated by using Pople's dipolar equation[57] ($\mu_\perp$ is the perpendicular dipole of a benzene ring) from structures generated with CHARMM in which the cant was varied every 5° for three tilt values (90°, 75°, 60°). A dimensionally correct shielding cone is superimposed on the molecule (C–S–C = 104°) which is shown in the (75°, 0°) configuration. Protons 2-H, 3-H, and 4-H reside inside the shielding cone (+), while 5-H and 6-H are deshielded (−).

values are differences in shifts of a given proton in a hexakis(arylthio)benzene and a suitable reference compound A, B, or C. The differences remove the intrinsic electronic and shielding properties of the substituent aryl ring to which the proton is attached. Consequently, the shielding effects arise from the central ring and its other substituents and provide a probe into the conformational freedom of the molecules in Table VII, which includes ligands **1**–**3**. The shielding values represent dynamic averages over multiple configurations because the NMR time scale is orders of magnitude slower than the motions that vary the shielding contributions.[54]

A sense of the relationship of cant and tilt angle to the magnitude of the shielding of 2-H in hexakis(arylthio)benzenes can be obtained from the behavior of 2-H in diphenyl sulfide. As shown in Figure 12, the molecular conformation is specified by the tilt and cant angles (θ, ϕ). Significant shielding or deshielding of 2-H occurs only in one-third of the cant range ($-60° \leq \phi \leq 60°$). Shielding rises to a maximum near cant angles of 0°, where 2-H is directed inward. In other regions, this proton experiences only slight deshielding. Energy minimization of diphenyl sulfide with the CHARMM force field predicts that the most stable conformation is (90°, 90°), with (90°, 0°) only 0.8 kcal/mol higher in energy. The slight deshielding observed for the 2-H proton of this molecule (Table VII) is not surprising.[55]

Molecules **7** and **8** have the least structural complexity of any of the hexakis(arylthio)benzenes in Table VII, and thus provide baselines for comparison. The atom numbering scheme in Figure 1 applies to all compounds in the table. In **7**, the shielding of 2,6-H is 0.32 ppm, the minimum in the set for these protons. When in the ababab conformation, the substituents are sufficiently separated that the source of shielding is primarily the central ring.[56] Introduction of a 6-Me group increases the 2-H shielding to 0.55 ppm. An inward projection of the methyl group, over the central ring, is sterically unfavorable. Consequently, the 2-H proton predominantly resides in this inward position. In the remaining molecules in Table VII, larger shielding of a particular proton implies a greater tendency of that proton to be directed inward, into the shielding cone of the central ring.

Consistent trends are evident in the shielding data for trithiols **1**–**3** and **9** and their respective protected forms **1p**–**3p** and **9p**. Molecules **2**, **3**, and **9** provide special insight into populated conformations because protons 2-H and 6-H simultaneously sample environments on both sides of their phenyl rings. Several observations are of particular importance. (i) Shielding of 2-H is always larger than 6-H in the set **2**, **3**, and **9** and is largest with ligand **2**.[58] (ii) Deprotection of thiol groups results in increased 2-H shielding in **1**–**3** and **9**, the order being **1** > **2** > **3** > **9**. The basis of these effects is steric in origin. The ring substituents 6-Me (**1**, **1p**) and 5-*t*-Bu (**2**, **2p**) favor conformations in which these groups are directed outward from the central ring. Similarly, deprotection of thiol groups results in an increase in shielding of 2-H; inward projection of the three 3-SCH_2OMe groups is sterically difficult whereas three thiol groups are readily accommodated. However, not all protected molecules have the same average conformation. Molecules **3p** and **9p**, lacking steric directing groups at the 5- or 6-position, maintain a conformation in which the 3-SCH_2OMe groups are directed outward, as seen from shielding order 6-H > 2-H. This differs from the case of

(53) The assignments of proton chemical shifts of compounds in this table are available as supplementary material. These were based primarily on intensities and spin–spin couplings. Ambiguities were resolved by spin-decoupling, 2-D methods, and/or analogies to previously assigned compounds.
(54) Hoch, J. C.; Dobson, C. M.; Karplus, M. *Biochemistry* **1982**, *21*, 1118.
(55) On the NMR time scale, 2-H and 6-H of diphenyl sulfide are equivalent. The correlated positioning of these protons on a single ring ($|\phi|_{2\text{-H}} = |\phi - 180°|_{6\text{-H}}$) in any one particular configuration will attenuate the positive shielding effect.
(56) This conclusion results from an analysis of shielding by a molecular dynamics calculations (vide infra). A configuration of 50 ps trajectory of **8** was analyzed by using Pople's equation[57] to calculate the shielding effects. Of the total calculated shielding of the 2-H proton (0.32 ppm), 90% was derived from the central ring and 10% from the other aryl substituents.
(57) Pople, J. A. *J. Chem. Phys.* **1956**, *24*, 1111.
(58) The chemical shifts of the 6-H proton of **3** and **9** are actually slightly smaller than those of the 2-H protons in the same molecules. The conclusion that the latter protons experience greater shielding results from the use of compound B_1 as a reference (Table VII; cf. supplementary material[30]).

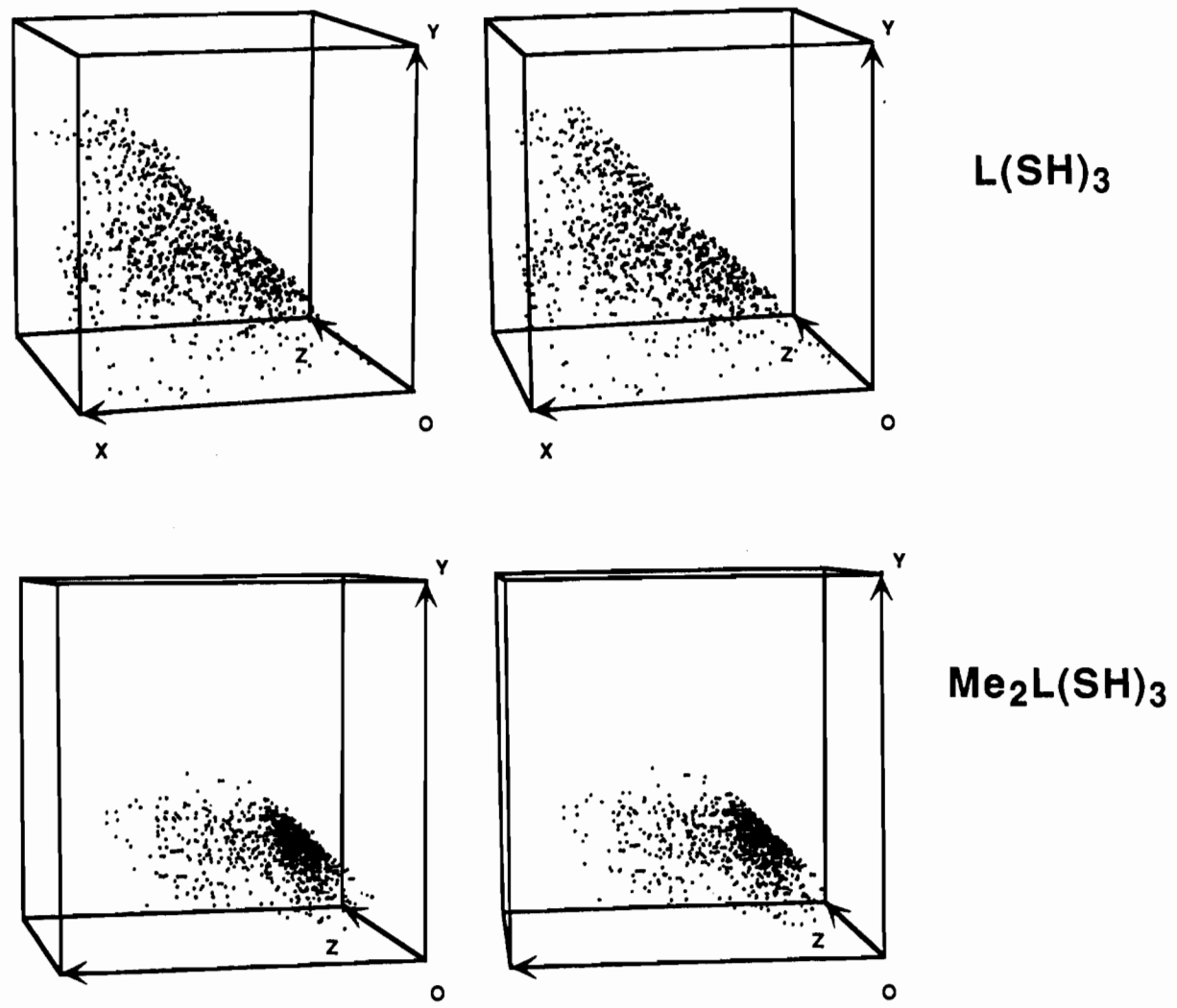

Figure 13. Stereoviews of 1000 configurations of **1** and **3** as defined by the absolute values of the cant angles ϕ of the three arms. Each point represents a single configuration calculated every 100 fs. Each axis runs from 0 to 180°. Only one-sixth of the volume is occupied owing to the sorting of the three angles into maximum (x axis), intermediate (y axis), and minimum (z axis) values.

1p and **2p**, where the directing groups are sufficient to maintain the reverse shielding order. Even without directing groups, **3** and **9** predominantly orient the 3-SH group inward (shielding order 2-H > 6-H). However, the difference between the shielding of these protons in **3** (0.12 ppm) and **9** (0.09 ppm) is considerably smaller than that found for **2** (0.35 ppm). The collective data demonstrate that average conformations are affected by ring substituents and strongly suggest that ligands **1** and **2** are more predisposed towards tridentate binding of a single cubane than is **3**.

(b) Molecular Dynamics. While shielding effects are useful in indicating dominant average conformations, they do not provide any insight into the spatial correlation of the coordinating arms of the ligands. The origin of the correlation is steric in nature. To examine this configurational aspect, molecular dynamics calculations were performed on ligands **1** and **3** by using the program CHARMM.[59] An analysis of these calculations yields information on the interaction of the coordinating arms and affords a better sense of the greater predispostion of **1** than **3** toward binding a single cubane. Because the molecules remained in the ababab conformation throughout the durations of the trajectories, the tilt angles varied only slightly from the mean value $\theta = 90°$.[61]

Table VIII. Average Cant Angles (deg) and Configurations (%) of Ligands **1** and **3** for 100-ps Trajectory

property		1	3
max cant angle		67	93
interm cant angle		46	73
min cant angle		37	43
		% confign	
		1	3
confign[a]	ϕ = 70°	ϕ = 90°	ϕ = 70°	ϕ = 90°
iii	71	87	31	49
iio	29	13	21	16
ioo	0	0	35	31
ooo	0	0	13	4

[a] Key: i, inward; o, outward.

(59) Brooks, R. B.; Bruccoleri, R. E.; Olafson, B. D.; States, D. J.; Swaminathan, S.; Karplus, M. *J. Comput. Chem.* **1983**, *4*, 187. The calculations employed the most recent (1988) all-atom force field including explicit charges. The parametrization of the sulfur atoms linking substituents to the central ring was derived from the parameters of methionine or cysteine. A C–S bond distance of 1.775 Å and a C–S–C bond angle of 104° were used; these values were taken from the structures of unhindered diaryl sulfides.[60] Trajectories were calculated after the molecules were minimized in energy with a bulk dielectric constant of 5 (approximately that of $CHCl_3$) and then heated to 300 K over 3 ps and equilibrated at that temperature for 5 ps. The coordinates of the molecular configuration were recorded every 10 fs from which the chemical shifts were calculated by using the dipolar equation of Pople.[57]

(60) (a) Andretti, G. D. *Cryst. Struct. Commun.* **1981**, *10*, 789. (b) Rozsondai, B.; Moore, J. H.; Gregory, D. C.; Hargittai, I. *Acta Chim. Hung.* **1977**, *94*, 321.

(61) Two sets of results from the molecular dynamics calculations of **1** and **3** are available as supplementary material:[30] a plot of the distributions of tilt angles (which peak more sharply at 90° for **1** than for **3**); a plot of the maximum magnitude cant angle vs the intermediate magnitude cant angle from 100-ps trajectories.

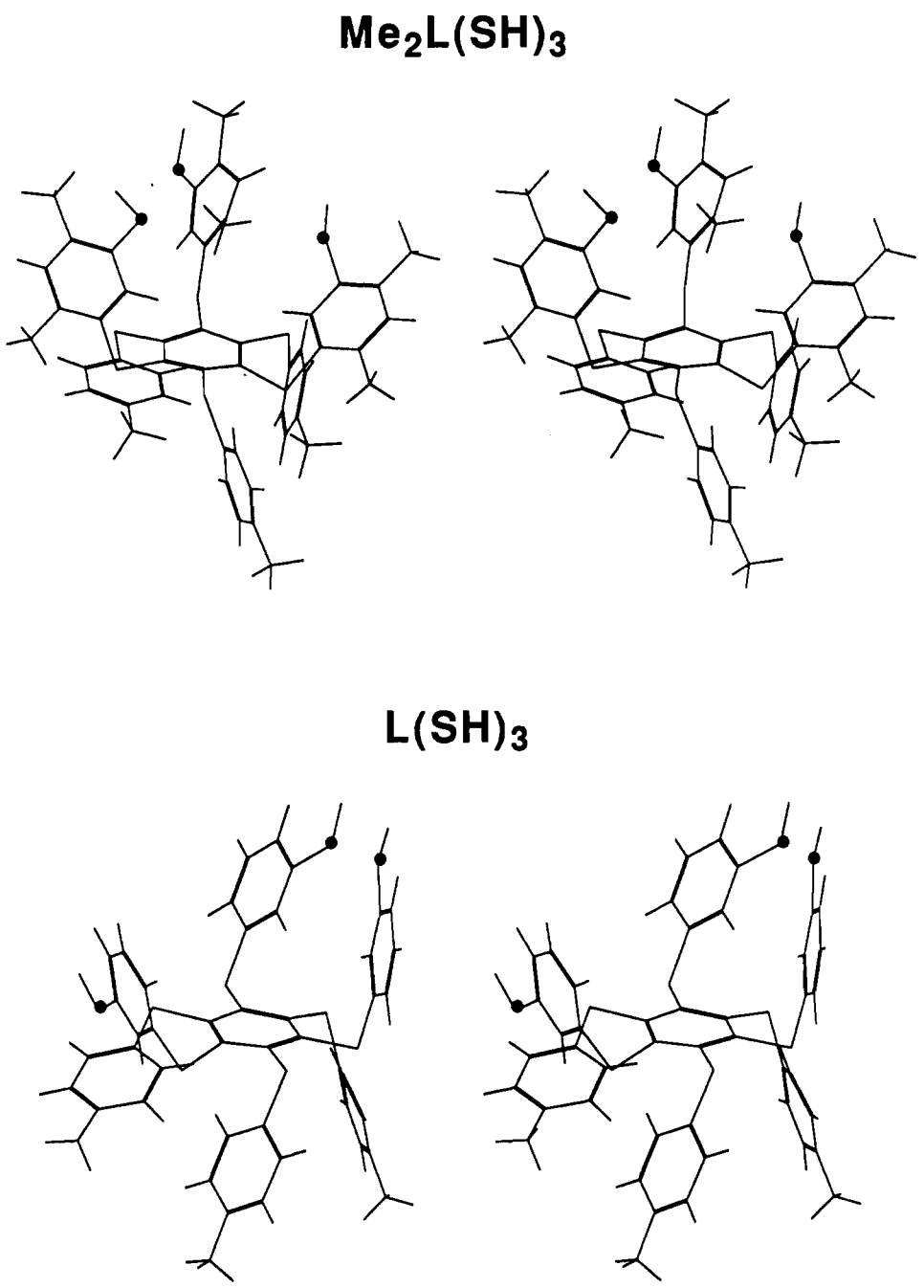

Figure 14. Stereoviews of a favorable cluster binding configuration of ligand **1** (iii; three cant angles with $\phi < 90°$; actual values 63, 52, 36°) and an unfavorable binding configuration of ligand **3** (ioo; two cant angles with $\phi > 90°$; actual values 143, 122, 63°).

Therefore, any large differences in configuration within the overall ababab conformation will be set by the three cant angles of the arms.

Shown in Figure 13 are stereoviews of two scatter plots of the calculated configurations of 100-ps trajectories of **1** and **3**. Each configuration is plotted in terms of its maximum (x axis), intermediate (y axis), and minimum (z axis) cant angle.[61] The averages of the three angles for 10000 configurations are presented in Table VIII; also given are the distribution of configurations with respect to an inward (i, $|\phi| < 70°$) or outward (o, $|\phi| > 70°$) projection of a substituent ring.[62] In the inward projection, 2-H and 3-SH are situated within the molecular cavity; in the outward projection, they are on the outside of the molecule. The restricted configurational freedom of the arms of **1** relative to **3** is immediately apparent.

The configurational distribution indicates that ligand **1**, with its greater population of the "all-in" (iii) configuration than ligand **3** (71% vs. 31%) is much more predisposed toward single cubane capture. Of equal or greater importance is that **1** *has no configurations in which more than one arm is rotated outward.* In contrast, 48% of the configurations of **3** have two or three arms rotated outward. Such outward configurations would cause the ligand to bind to more than one cluster, thus promoting polymerization. This is the dominant behavior of ligand **3**. Outward configurations are energetically unfavorable for **1** and **2** owing to steric interactions, particularly in the (ioo) and (ooo) arrangements. Provided in Figure 14 are stereoviews of a configuration (iii) of **1** illustrating predisposition toward binding and an unfavorable configuration of **3**. We conclude that the propensity of ligands **1** and **2** to capture a single cubane is dependent on a predisposition toward cavity formation and against polymerization. The actual substitution steps occur by proton transfer

(62) The choice of a cant angle that delineates an inward from an outward projection is somewhat arbitrary. The intuitive choice would be 90°, but an all-90° configuration does not have the appearance of being predisposed to cluster capture as much as an all-70° configuration.

from the arenethiol groups to the alkanethiolate ligands of a cluster such as $[Fe_4S_4(SEt)_4]^{2-}$.[63] We have also shown that cubane clusters are isolated in high yield from reactions employing the trianion of ligand **1** in Me_2SO solutions.[47] These results suggest that $(Me_2LS_3)^{3-}$ is predisposed to cluster capture in a manner similar to the protonated ligand.[64]

Interactions with Other Clusters. With the demonstration that ligands **1** and **2** bind essentially quantitatively to a cubane cluster, the question arises as to whether their flexibility is sufficient for them to bind as tridentates to clusters of other shapes. The only clusters currently available for such a test are the prismanes $[Fe_6S_6L_6]^{2-,3-}$ (**14**, L = halide, ArO^-).[65] Reaction of $[Fe_6S_6(OC_6H_4\text{-}p\text{-}Me)_6]^{3-}$ and 2 equiv of **1** in Me_2SO yielded one or more products whose ^1H NMR shifts are entirely consistent with the $[Fe_4S_4]^{2+}$ core.[2,13-15] The spectrum did not, however, correspond to $[Fe_4S_4(Me_2LS_3)(OC_6H_4\text{-}p\text{-}Me)]^{2-}$, which has been independently prepared by the reaction of cluster **4** and sodium cresolate.[13,66] The products have not been further identified. Additionally, reaction of $[Fe_6S_6Cl_6]^{3-}$ with 1 or 2 equiv of **1** (in the presence of 3 or 6 equiv of Et_3N) in acetonitrile gave **4** as the only product detectable by ^1H NMR.

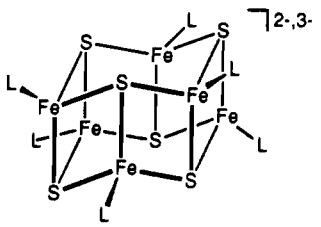

14

Only cubane-type products have been identified from the reactions of prismanes and ligand **1**. The prismane cluster presents two faces to an attacking ligand: an Fe_3S_3 ring whose Cl···Cl separations are 7.3 Å and two fused Fe_2S_2 rhombs whose Cl···Cl separations are two at 5.5 Å and one at 7.3 Å. These may be too demanding of ligand flexibility, which in four $[Fe_4Q_4]^{2+}$ structures (**4**, **5**) is required to span S···S distances of 6.42-6.67 Å.

Acknowledgment. This research was supported by NIH Grant GM 28856. X-ray equipment was obtained through NIH Grant 1 S10 RR 02247. We thank Professor M. Karplus and Dr. J. R. Smith for useful discussions and Dr. G. Henkel for permission to quote structural results prior to publication.

Supplementary Material Available: Crystallographic data for $(Ph_4P)_2[Fe_4Se_4(Me_2LS_3)Cl]\cdot 2DMF$, including tables of intensity collection and structure refinement parameters, temperature factors, interatomic distances and angles, and positional parameters including hydrogen atoms, a table of chemical shifts of compounds in Table VII and others used in establishing assignments, and plots of tilt angle distributions and maximum vs intermediate cant values for configurations of **1** and **3** from molecular dynamics calculations (19 pages); a table of structure factors (49 pages). Ordering information is given on any current masthead page.

(63) Dukes, G. R.; Holm, R. H. *J. Am. Chem. Soc.* **1975**, *97*, 528.

(64) While we have not attempted to evaluate the shielding of 2-H in $(Me_2LS_3)^{3-}$ with the use of anionic reference compounds, its chemical shift (6.49 ppm in Me_2SO) is very close to that of **1** (6.45 ppm in $CDCl_3$) at 297 K. Other chemical shifts of the trianion are as follows: δ 1.82 (4-Me), 2.05 (6-Me), 2.24 (4′-Me), 6.79 (5-H), 6.80 (3′-H), 7.05 (2′-H). Ligand **1** is not soluble in Me_2SO, so that a direct comparison of shifts in the same solvent is not available.

(65) (a) Coucouvanis, D.; Kanatzidis, M. G.; Dunham, W. R.; Hagen, W. R. *J. Am. Chem. Soc.* **1984**, *106*, 7998. (b) Kanatzidis, M. G.; Hagen, W. R.; Dunham, W. R.; Lester, R. K.; Coucouvanis, D. *J. Am. Chem. Soc.* **1985**, *107*, 953. (c) Kanatzidis, M. G.; Salifoglou, A.; Coucouvanis, D. *Inorg. Chem.* **1986**, *25*, 2460.

(66) Chemical shifts: reaction product, δ 8.10 (5-H), 3.83 (6-Me), 3.60 (4-Me) (main signals of the arms); authentic $[Fe_4S_4(Me_2LS_3)(OC_6H_4\text{-}p\text{-}Me)]^{2-}$, δ 8.77 (m-H), 8.23 (5-H), 4.66 (p-Me), 3.95 (6-Me), 3.71 (4-Me).

Contribution from the Department of Chemistry,
The University of North Carolina, Chapel Hill, North Carolina 27599-3290

Synthesis, Structure, and Redox Properties of the Triaqua(tris(1-pyrazolyl)methane)ruthenium(II) Cation

Antoni Llobet,[1a] Derek J. Hodgson,[1b] and Thomas J. Meyer*[,1c]

Received August 15, 1989

The synthesis of the salt $[(tpm)Ru(H_2O)_3](p\text{-}CH_3C_6H_4SO_3)_2\cdot 1.5H_2O$, where tpm is the terdentate facial ligand tris(1-pyrazolyl)methane, is described. The salt was prepared as a possible precursor to a structurally stabilized but reactive *cis*-dioxoruthenium(VI) oxidant. The crystal structure of the salt has been determined from three-dimensional X-ray data. It crystallizes in the triclinic space group $P\bar{1}$ with two formula units in a cell of dimensions a = 10.780 (5) Å, b = 11.122 (8) Å, c = 14.489 (4) Å, α = 74.60 (5)°, β = 67.23 (4)°, and γ = 87.41 (5)°. The structure has been refined to a final value of R = 0.031 based on the intensities of 3390 reflections. The crystal structure proves that the complex is the *fac* isomer in which the terdentate ligand occupies three sites on one face of the coordination octahedron and the three water molecules occupy the opposite face. Electrochemical studies at activated glassy-carbon electrodes show the appearance of waves for Ru(III/II), Ru(IV/III), and Ru(V/IV) couples. Oxidation past Ru(IV) leads to an opening of one of the chelating arms of the tpm ligand and formation of a *trans*-dioxo complex of Ru(VI).

Introduction

For complexes of osmium and ruthenium a diverse higher oxidation state chemistry exists based on metal-oxo formation.[2-5] Characteristically, the higher oxidation states can be reached by sequential oxidation and proton loss from lower oxidation state

(1) (a) Fulbright "La Caixa" Fellow, Barcelona, Spain. Permanent address: Department de Quimica (Area 10), Universitat Autonoma de Barcelona, 08193 Bellaterra, Barcelona, Spain. (b) Department of Chemistry, University of Wyoming. (c) Department of Chemistry, The University of North Carolina.

(2) (a) Moyer, B. A.; Meyer, T. J. *J. Am. Chem. Soc.* **1978**, *100*, 3601. (b) Moyer, B. A.; Meyer, T. J. *Inorg. Chem.* **1981**, *20*, 436. (c) Pipes, D. W.; Meyer, T. J. *J. Am. Chem. Soc.* **1984**, *106*, 7653. (d) Gilbert, J. A.; Eggleston, D. S.; Murphy, W. R., Jr.; Geselowitz, D. A.; Gersten, S. W.; Hodgson, D. J.; Meyer, T. J. *J. Am. Chem. Soc.* **1985**, *107*, 3855. (e) Gilbert, J. A.; Geselowitz, D. A.; Meyer, T. J. *J. Am. Chem. Soc.* **1986**, *108*, 1493. (f) Pipes, D. W.; Meyer, T. J. *Inorg. Chem.* **1986**, *25*, 4042. (g) Doppelt, P.; Meyer, T. J. *Inorg. Chem.* **1987**, *26*, 2027.

0020-1669/90/1329-3760$02.50/0